# Jet evolution in the $\mathcal{N} = 4$ SYM plasma at strong coupling

**Y. Hatta**

*Graduate School of Pure and Applied Sciences, University of Tsukuba, Tsukuba, Ibaraki 305-8571, Japan*
*E-mail:* `hatta@het.ph.tsukuba.ac.jp`

**E. Iancu**

*Institut de Physique Théorique de Saclay, F-91191 Gif-sur-Yvette, France*
*E-mail:* `Edmond.Iancu@cea.fr`

**A. H. Mueller**

*Department of Physics, Columbia University, New York, NY 10027, USA*
*E-mail:* `amh@phys.columbia.edu`

ABSTRACT: Within the framework of the AdS/CFT correspondence, we study the time evolution of an energetic $\mathcal{R}$–current propagating through a finite temperature, strongly coupled, $\mathcal{N} = 4$ SYM plasma and propose a physical picture for our results. In this picture, the current splits into a pair of massless partons, which then evolve via successive branchings, in such a way that energy is quasi–democratically divided among the products of a branching. We point out a duality between the transverse size of the partonic system produced through branching and the radial distance traveled by the dual Maxwell wave in the AdS geometry. For a time–like current, the branching occurs already in the vacuum, where it gives rise to a system of low–momentum partons isotropically distributed in the transverse plane. But at finite temperature, the branching mechanism is modified by the medium, in that the rate for parton splitting is enhanced by the transfer of transverse momentum from the partons to the plasma. This mechanism, which controls the parton energy loss, is sensitive to the energy density in the plasma, but not to the details of the thermal state. We compute the lifetime of the current for various kinematical regimes and provide physical interpretations for other, related, quantities, so like the meson screening length, the drag force, or the trailing string, that were previously computed via AdS/CFT techniques.

## Contents

## 1. Introduction

Motivated by some experimental results from the heavy ion program at RHIC, which suggest that the deconfined, 'quark–gluon', matter produced in the early stages of an ultrarelativistic nucleus–nucleus collision might be strongly interacting (see, e.g., the review papers [1, 2] and references therein), there was recently an abondance of applications of the AdS/CFT correspondence to problems involving a strongly–coupled gauge plasma at finite temperature and/or finite quark density (for a recent review see [3]). While the early such applications have focused on the long–range and large–time properties of the plasma, so like hydrodynamical flow and transport coefficients, more recent studies have been also concerned with the response of the plasma to a 'hard probe' — an energetic 'quark' or 'current' which probes the plasma on very short time and distance scales, much shorter than the thermal scale $1/T$ (with $T$ being the temperature). Although the relevance of such applications to actual hard probes in QCD is perhaps not so clear (since, by asymptotic freedom, QCD should be weakly coupled on such short space–time separations), the results that have been obtained in this way are conceptually interesting, in that they shed light on a new physical regime — that of a gauge theory with strong interactions — which for long time precluded all first–principles theoretical investigations other than lattice

gauge theory. For these results to be accompanied by conceptual clarifications, a physical interpretation for them is strongly needed, but this seems to be difficult without direct calculations in the original gauge theory. A different strategy, which is less rigorous, is to propose a physical picture based on general arguments and then demonstrate that this picture is consistent with all the available results (to the extent that comparisons are possible). This will be our strategy in this paper.

The physical problem that we shall consider — the propagation of an 'electromagnetic' current (actually, an $\mathcal{R}$–current) through the plasma — is particularly well suited for our purposes since, first, it has a strong overlap with several other problems previously considered in the literature and, second, it does not require any extension of the AdS/CFT correspondence (like the introduction of additional D7–branes) beyond the 'minimal' framework of its original formulation [4, 5, 6] — so it avoids any potential artifact due to such extensions. Besides, this problem has another useful feature: for the gauge theory of interest — namely, the conformally invariant $\mathcal{N} = 4$ supersymmetric Yang–Mills (SYM) theory — the current–current correlator in the vacuum (or 'vacuum polarization tensor') is protected by supersymmetry [7], in such a way that the full result in the strong 't Hooft coupling limit $\lambda \equiv g^2 N_c \to \infty$ is exactly the same as the corresponding result in lowest–order perturbation theory (i.e., the one–loop approximation). This property will allow us to recognize — via a comparison between the space–time picture of the one–loop process in the gauge theory and the 'supergravity' picture of the dual AdS/CFT calculation — an interesting 'duality' between the physical transverse size of the partonic system into which the current is evolving and the radial distance in $AdS_5$. In turn, this duality will be a key ingredient of our proposal for a physical interpretation.

Specifically, we shall follow the time–evolution of an $\mathcal{R}$–current which in the plasma rest frame propagates like a plane–wave in the $z$ direction, with a large longitudinal momentum $q \gg T$ and frequency $\omega \simeq q$, and which at $t = 0$ has zero transverse size. At weak coupling, this current would develop a partonic fluctuation involving just two partons — massless fields from $\mathcal{N} = 4$ SYM which carry $\mathcal{R}$–charge and transform in the adjoint representation of the color group $SU(N_c)$. For a space–like current, this pair would grow in transverse space up to a maximal size $L \sim 1/Q$ and live for a relatively long time $t_c \sim q/Q^2$, thus acting like a 'color dipole' which can mediate the current interactions with an external target. (Here $Q^2 \equiv q^2 - \omega^2$ is the virtuality of the current, and is positive in the space–like case.) For a time–like current ($Q^2 < 0$), the pair can dissociate after a time $t \sim t_c$ and thus give rise to two free partons which separate from each other, so like the quark and antiquark jets produced in $e^+e^-$ annihilation. This perturbative, one–loop, picture formally applies also to the full vacuum polarization tensor at strong coupling, because of the non–renormalization property alluded to above. This explains the polyvalence of the $\mathcal{R}$–current as a 'hard probe', including at strong coupling[1] : by tuning the virtuality and the momentum of the current, we can mimic a color dipole, a 'meson', or a pair of jets with the desired values for the system size and rapidity, and then study the interactions between this partonic system and the plasma (or any other target).

But, of course, all that applies to a current propagating through the vacuum, and there is *a priori* no guarantee that a similar strategy should also work in the thermal bath. In a previous

---

[1]We should also mention here the use of the current in the calculation of the rate for 'photons' or 'dileptons' production in the $\mathcal{N} = 4$ SYM plasma at strong coupling [8].

analysis [9], we have considered the case of a space–like current — i.e., the problem of deep inelastic scattering off the plasma — and shown (via the appropriate AdS/CFT calculation) that this strategy still works, but only for not too high energies. A current with relatively low energy, such that $q \ll Q^3/T^2$, propagates through the plasma essentially without interacting, so like a 'small meson' in the approach of Refs. [10, 11, 12, 13, 14, 15], where the 'meson' was made with two 'heavy quarks' attached to a D7–brane. Note that the above condition on $q$ can be rewritten as a lower bound on the current virtuality, $Q \gg Q_s$, with $Q_s \sim (qT^2)^{1/3}$ the plasma saturation momentum, and also as an upper bound on the transverse size of the effective dipole, $L \ll 1/Q_s$, which is then consistent with the respective bound (the 'meson screening length') found in Refs. [10, 11, 12].

But for higher energies $q \gtrsim Q^3/T^2$, or, equivalently, lower virtualities $Q \lesssim Q_s$, the analysis of Ref. [9] shows that the current is very rapidly absorbed into the plasma, over a time $t_s \sim q/Q_s^2(q) \propto q^{1/3}$ which is much shorter than the period $t_c \sim q/Q^2$ required for the formation of a nearly on–shell partonic fluctuation. That is, for such a high energy, the current cannot be assimilated with a color dipole anymore (not even over a finite period of time), as it disappears before a dipole can form. The above result on $t_s$ can be restated by saying that the current propagates through the plasma over a longitudinal distance $z_s \propto q^{1/3}$ before it disappears. Interestingly, the same parametric estimate has been very recently found for the penetration length of an effective gluon [16]. In view of the physical picture that we shall develop, this similarity is not just a coincidence, but rather it reflects the universality of the dissipation mechanism in the strongly–coupled plasma.

In Ref. [9], the current lifetime $t_s$ has been inferred from physical considerations, but no temporal evolution (on top of the usual phase $\mathrm{e}^{-i\omega t}$ from the definition of the plane–wave) was explicitly considered. In this paper we shall extend that analysis by addressing the time–dependent problem, for both space–like and time–like currents, with the purpose of elucidating the dynamics of the current and the mechanism responsible for its dissipation. As already mentioned, we shall consider initial conditions such that the current has zero transverse size at $t = 0$. In the dual string calculation, this is represented by a vector field propagating in the $AdS_5$–Schwarzschild metric which at $t = 0$ is localized at the Minkowski boundary $r \to \infty$ of $AdS_5$. For $t > 0$, this perturbation propagates inside the bulk of the '5th dimension' as a Maxwell wave, i.e., according to the Maxwell equations in the $AdS_5$–Schwarzschild geometry. For the kinematics of interest, these equations can be suggestively rewritten in the form of time–dependent Schrödinger equations, to be presented in Sect. 2.

We first analyze the zero–temperature case (in Sect. 3), where the relevant geometry is purely $AdS_5$. By solving the 'Schrödinger equations' in the approximations of interest and comparing the results to the space–time picture of the quantum fluctuation of the current into a pair of massless fields, we find that the two pictures match indeed with each other after provided one identifies the radial dimension $r$ in $AdS_5$ with the inverse $1/L$ of the transverse size of the partonic fluctuation: more precisely, $R^2/r \leftrightarrow L$, wit $R$ the curvature radius for $AdS_5$. For instance, on the supergravity side, the temporal scale $t_c \sim q/Q^2$ appears as the time after which the wave has penetrated into the bulk up to a distance $r \sim R^2Q$. This corresponds, on the gauge theory side, to the fact that the partonic fluctuation requires a formation time $t_c \sim q/Q^2$ in order to grow up to a transverse size $L \sim 1/Q$. Notice that this formation time is a genuine quantum

effect, which reflects the uncertainty principle. This suggests that, for the problem at hand, the 5th dimension of $AdS_5$ somehow mimics, within the context of the classical supergravity calculation, the phase–space for physical quantum fluctuations in transverse space.

This $r \leftrightarrow L$ duality helps us identify a physical picture for the current dynamics in the vacuum. The naive one–loop picture (2–parton fluctuation) cannot be right at strong coupling, where any of the two partons produced in the original splitting of the current can further radiate, or scatter off the vacuum fluctuations. Quantum field are known for their strong propension to radiation. When the coupling is weak, the radiation is concentrated in specific corners of the phase space (collinear and soft radiation for a gauge theory), where the smallness of the coupling is compensated by the phase–space available to radiation. This leads, e.g, to the celebrated DGLAP and BFKL evolution equations in perturbative QCD. But at strong coupling, there is no reason why radiation should be restricted to small corners of phase–space; this should most naturally proceed via the 'democratical' branching of the original quanta into two daughter partons with more or less equal shares of their parent energy and momentum. We therefore propose a physical picture for current (or parton) evolution a strong coupling (and in the vacuum) in terms of successive branchings, such that the energy and the virtuality are divided by two (for simplicity) at each individual branching, and that the lifetime of a generation is determined by the formation time for the next generation, in agreement with the uncertainty principle. As we show in Sect. 5.2, this simple picture reproduces indeed the results of the respective AdS/CFT calculation, at a qualitative level.

Moving now to the finite–temperature case, we find (by solving the appropriate 'Schrödinger equations', in Sect. 4) that, for low and moderate energies, such that $q \ll Q^3/T^2$, and for not too large values of time, the dynamics remains essentially as in the vacuum. For a space–like current, this confirms the previous results in Ref. [9]: a 'small meson', with size $L \sim 1/Q$, survives almost unaltered in the plasma. (The 'meson' can decay via tunnel effect, but the decay rate is exponentially suppressed [9].) But for a time–like current, the vacuum–like evolution proceeds only up to a time $t_f \sim \sqrt{\gamma}/T$, with $\gamma = q/Q \gg 1$ the Lorentz factor of the current. At this time $t_f$, the 'current' — or, more precisely, the partonic system produced via its successive branching — has propagated inside the plasma over a longitudinal distance $z_f \sim \sqrt{\gamma}/T$ and has extended in transverse space up to a size $L_f \sim 1/\sqrt{\gamma}T$. Note that this value $L_f$ is precisely of the order of the meson screening length computed in Refs. [10, 11, 12], and more commonly written as $L_f \sim (1 - v^2)^{1/4}/T$, with $v$ the velocity of the meson. More detailed comparisons between our approach and previous results in the literature will be performed in Sect. 5.1.

For larger times $t \gtrsim t_f$, this partonic system starts interacting with the plasma, although its transverse size is still much smaller than $1/T$. In this regime, the dual string calculation shows that the Maxwell wave feels the attraction of the black hole and thus undergoes an accelerated fall towards the horizon, that it gets close to after a time of order $t_f$. When this radial dynamics is translated to transverse space, via the $r \leftrightarrow L$ duality mentioned before, it implies that the partons feel a constant, decelerating, force in the transverse directions,

$$\frac{\mathrm{d}p_\perp}{\mathrm{d}t} \sim -T^2 \,, \tag{1.1}$$

whose precise physical meaning remains a little mysterious to us (see the discussion in Sect. 5.2). By including the action of this force on the dynamics of branching, we will be able to show that

*medium–induced branching* is a likely physical scenario, which is qualitatively consistent with the results of the AdS/CFT calculation. By 'medium–induced branching' we mean that the change in virtuality over the lifetime of a partonic generation is due to the transfer of transverse momentum to the plasma, at a constant rate $\sim T^2$ (see Sect. 5.2 for more details).

The same physical scenario — an accelerated fall of the Maxwell wave into the black hole, which physically corresponds to medium–induced branching — holds also in the high–energy regime at $q \gtrsim Q^3/T^2$, for *both* space–like and time–like currents, but in this regime, this scenario starts to apply much earlier, after a time $t_s \sim q/Q_s^2(q)$ which is much shorter than the formation time $t_c \sim q/Q^2$ for an on–shell partonic fluctuation. (We recall that $Q_s \sim (qT^2)^{1/3}$ is the plasma saturation momentum.) Thus, such an energetic current disappears in the plasma before having the time to create 'jets' (on–shell partons). Within this scenario, we find a natural physical explanation for the 'drag force' experienced by partons in the plasma (originally computed for a heavy quark probe in Refs. [17, 18]), and also for the 'trailing string solution' (the string attached to an energetic heavy quark propagating through the plasma $AdS_5$–Schwarzschild geometry [17, 18]), that we recognize as the dual of the enveloping curve of the spatial distribution of partons produced through medium–induced branching. It remains as an interesting open problem to understand whether this scenario can naturally accommodate also other quantities computed within AdS/CFT, so like the jet quenching [19], or the transverse momentum broadening [20, 21].

One can succinctly summarize the previous discussion as follows: While a highly virtual (and hence very small) *space–like* 'meson', with virtuality $Q \gg Q_s(q)$, can survive in the strongly–coupled plasma (essentially without feeling the latter), this is not also the case for the jets produced by the decay of a highly virtual *time–like* current, which can only propagate over a longitudinal distance $z_f \sim \sqrt{\gamma}/T$ before disappearing in the plasma. Less virtual (or more energetic) partonic systems, for which $Q \ll Q_s(q)$, cannot form in the first place : the virtual partons melt in the plasma over a time $t_s \sim q/Q_s^2(q)$, which is too short to get on–shell. The dissipation mechanism is *universal*, i.e., the same for all kind of partons — off–shell or on–shell, massive or massless, quarks, scalars, or gluons — and it consists in medium–induced branching.

Let us conclude this Introduction with a remark concerning the spatial distribution of the hadrons produced via the decay of a time–like current in the vacuum. For the concept of hadron to make sense, we supplement the theory with an infrared cutoff $\Lambda$ and assume that the current is 'hard' relative to this cutoff : $|Q| \gg \Lambda$. Then the decay of the current via successive branchings will produce a system of $\sim |Q|/\Lambda$ hadrons with small transverse momenta $\sim \Lambda$, which are isotropically distributed in the transverse plane. (In the rest frame of the current, this distribution would be spherically symmetric.) This observation is the 'time–like' counterpart of a previous result that, at strong coupling, there are no large–$x$ partons (i.e., no partons carrying a sizeable fraction of the hadron longitudinal momentum) in the wavefunction of an energetic hadron [22, 23, 9]. Rather, all partons have fallen down at very small values of $x$ (smaller than $x_s \sim T/Q$ in the case of the $\mathcal{N} = 4$ SYM plasma [9] and, respectively, $x_s \sim (\Lambda/Q)^2$ for a hadron [23]), via successive branchings within space–like cascades. Because of that, a high–energy 'nucleus–nucleus' collision which would liberate these partons would produce no jets, but only a multitude of particles at central rapidity which are isotropically distributed in transverse space, with small momenta $p_\perp \sim \Lambda$. This picture is similar, and possibly related, to a very recent result [24] showing that the energy distribution of the particle produced in the strong–coupling analog

of the $e^+e^-$ annihilation exhibits spherical symmetry. On the other hand, this picture looks quite different from the corresponding one in perturbative QCD and also from the respective results for nucleus–nucleus collisions at RHIC.

## 2. General equations

We would like to address the following physical problem: at time $t = 0$, an $\mathcal{R}$–current with momentum $q$ oriented along the $z$ axis and energy $\omega$ acts in the $\mathcal{N} = 4$ SYM plasma, producing a system of SYM quanta which then propagate through the plasma until they finally disappear. In the dual gravity problem, this current dynamics is represented by the propagation of a Maxwell–like gauge field $A_m$ in the background geometry of the $AdS_5$ black hole (representing the $\mathcal{N} = 4$ SYM plasma) [3]. The corresponding metric reads

$$\mathrm{d}s^2 = \frac{(\pi TR)^2}{u}(-f(u)\mathrm{d}t^2 + \mathrm{d}\boldsymbol{x}^2) + \frac{R^2}{4u^2 f(u)}\mathrm{d}u^2 \,, \tag{2.1}$$

where $T$ is the temperature of the black hole (the same as for the $\mathcal{N} = 4$ SYM plasma), $R$ is the curvature radius of $AdS_5$, $t$ and $\boldsymbol{x} = (x, y, z)$ are the time and, respectively, spatial coordinates of the physical Minkowski world, $u$ is the radial coordinate on $AdS_5$, and $f(u) = 1 - u^2$. Note that our radial coordinate has been rescaled in such a way to be dimensionless: in terms of the more standard, dimensionfull, coordinate $r$, it reads $u \equiv (r_0/r)^2$, with $r_0 = \pi R^2 T$. Hence, in our conventions, the black hole horizon lies at $u = 1$ and the Minkowski boundary at $u = 0$.

Since the radial component $A_u$ vanishes at $u = 0$, it is possible and convenient to work in the gauge where $A_u$ is identically zero. Then, the non–zero components $A_\mu$, with $\mu = 0, 1, 2, 3$, are of the form:

$$A_\mu(t, \boldsymbol{x}, u) = \mathrm{e}^{-i\omega t + iqz} \, \tilde{A}_\mu(t, u) \,, \tag{2.2}$$

where $\tilde{A}_\mu(t, u)$ has a relatively weak time dependence, such that $|\partial_t \tilde{A}_\mu|/\tilde{A}_\mu \ll \omega$, and obeys the initial condition that, for $t \to 0$, $\tilde{A}_\mu(t, u)$ is localized near $u = 0$. (The precise structure of the initial condition is not really needed.) The relevant equations of motion are the Maxwell equations in the $AdS_5$ Schwarzschild geometry. They are most conveniently written as a set of equations for the transverse components $\tilde{A}_i$, with $i = 1, 2$, and, respectively, the longitudinal component $a(u) \equiv \partial_u A_0(u)$ (the $z$ component $A_z$ is not independent, but it is related to $A_0$ via the equations of motion), and read [3]

$$A_i'' + \frac{f'}{f}A_i' - \frac{1}{uf^2}\left(k^2 f + \frac{\partial^2}{\partial \tilde{t}^2}\right)A_i = 0 \tag{2.3}$$

and, respectively,

$$a'' + \frac{(uf)'}{uf}\,a' - \frac{1}{uf^2}\left(k^2 f + \frac{\partial^2}{\partial \tilde{t}^2}\right)a = 0\,, \tag{2.4}$$

where a prime on a field indicates a $u$–derivative and we have introduced the following, dimensionless, variables

$$\varpi \equiv \frac{\omega}{2\pi T}\,, \qquad k \equiv \frac{q}{2\pi T}\,, \qquad \tilde{t} \equiv 2\pi T t\,, \qquad \tilde{z} \equiv 2\pi T z\,. \tag{2.5}$$

(The variables $\varpi$ and $\tilde{z}$ will be used later on.) The above equations can be further simplified for our present purposes. First, as already mentioned, the field $\tilde{A}_\mu(t, u)$ is slowly varying in time; hence we can write

$$\frac{\partial^2}{\partial \tilde{t}^2} A_\mu \approx \mathrm{e}^{-i\varpi\tilde{t}+ik\tilde{z}} \left( -\varpi^2 - 2i\varpi \frac{\partial}{\partial \tilde{t}} \right) \tilde{A}_\mu \,, \tag{2.6}$$

where we have neglected the second–order time derivative of $\tilde{A}_\mu$. Furthermore, as we shall see, the interesting dynamics happens near to the boundary at $u = 0$ (and hence far away from the horizon at $u = 1$), so we can replace $f \to 1$ in the coefficients of the above equations everywhere except in the term $k^2 f = k^2(1 - u^2)$ : indeed, in that term, the small quantity $u^2 \ll 1$ can be amplified by the longitudinal momentum $k^2$ of the incoming current, which becomes very large at high energy. Notice that this term $k^2 u^2 = k^2(r_0/r)^4 \propto k^2 T^4/r^4$ represents the potential for the long–range (in $r$) gravitational interaction between the current and the black hole. Since we keep only this particular medium effect in our equations, but neglect those which would signal the black–hole singularity at $u = 1$ (the gravity–dual hallmark of a thermal system), we expect our subsequent results to apply to matter distributions more general than a finite–temperature plasma: similar results should hold for any matter distribution which is infinite and homogeneous (say, a cold matter), after replacing the energy density $\Theta_{00} \propto N_c^2 T^4$ of the finite–temperature plasma by the corresponding quantity for the cold matter.

After these simplifications, we end up with the following equations for $\tilde{A}_i$ and $\tilde{a}$, valid when $u \ll 1$ :

$$\begin{aligned} 2i\varpi \frac{\partial}{\partial \tilde{t}} \tilde{A}_i &= -u\tilde{A}_i'' \pm K^2 \tilde{A}_i - k^2 u^2 \tilde{A}_i \,, \\ 2i\varpi \frac{\partial}{\partial \tilde{t}} \tilde{a} &= -u\tilde{a}'' - \tilde{a}' \pm K^2 \tilde{a} - k^2 u^2 \tilde{a} \,, \end{aligned} \tag{2.7}$$

where we have introduced the notation $K^2 \equiv |k^2 - \varpi^2|$ and the plus (minus) sign in front of $K^2$ corresponds to a space–like (time–like) current. Note that, with its above definition, $K^2$ is always a positive quantity.

It will be furthermore useful (especially in view of constructing approximate solutions) to rewrite these equations in a form which resembles the time–dependent Schrödinger equation. To that aim, we shall perform the following changes of variable and functions:

$$\chi \equiv 2\sqrt{u}, \qquad \tilde{a}(\tilde{t}, u) \equiv \frac{1}{\sqrt{\chi}} \psi(\tilde{t}, \chi), \qquad \tilde{A}_i \equiv \sqrt{\chi}\, \phi_i(\tilde{t}, \chi) \,. \tag{2.8}$$

Also, we shall be mostly interested in the high energy regime where $\omega \simeq q \gg Q$, meaning $\varpi \simeq k \gg K$, so that we can replace $\varpi \simeq k$ in the coefficients of the equations. Then our final equations, valid for high energy and $\chi \ll 1$, read

$$i\frac{\partial \phi_i}{\partial \tilde{t}} = \left( -\frac{1}{2k} \frac{\partial^2}{\partial \chi^2} + \frac{3}{8k\chi^2} \pm \frac{K^2}{2k} - \frac{k\chi^4}{32} \right) \phi_i \,, \tag{2.9}$$

$$i\frac{\partial \psi}{\partial \tilde{t}} = \left( -\frac{1}{2k} \frac{\partial^2}{\partial \chi^2} - \frac{1}{8k\chi^2} \pm \frac{K^2}{2k} - \frac{k\chi^4}{32} \right) \psi \,. \tag{2.10}$$

To avoid a proliferation of cases, we shall mostly focus on the longitudinal case, cf. Eq. (2.10).

As anticipated, we choose initial conditions such that, at $t = 0$, the fields are localized near $u = 0$ (i.e., $\chi = 0$). We shall implement that by working in Fourier space; we thus write, e.g.,

$$\psi(\tilde{t}, \chi) = \int d\varepsilon \, e^{-i\varepsilon\tilde{t}} \, \psi(\varepsilon, \chi), \qquad (2.11)$$

where $\psi(\varepsilon, \chi)$ is a wave packet in $\varepsilon$ peaked around $\varepsilon = 0$. For convenience, we shall take this wave packet to be modulated by a Gaussian, that is,

$$\psi(\tilde{t}, \chi) = \int d\varepsilon \, e^{-i\varepsilon\tilde{t} - \frac{\varepsilon^2}{2\sigma^2}} \, \Psi(\varepsilon, \chi), \qquad (2.12)$$

where the width $\sigma$ is constrained by

$$k \gg \sigma \gg \frac{K^2}{k} \qquad (2.13)$$

and the additional $\varepsilon$–dependence in $\Psi(\varepsilon, \chi)$ will be fixed by Eq. (2.10). The first inequality in Eq. (2.13) ($k \gg \sigma$) ensures that the typical energy fluctuations obey $\varepsilon \ll \varpi \simeq k$, as originally assumed. The second inequality ($\sigma \gg K^2/k$) is necessary to allow for quasi–localized configurations in the initial condition and at early times (see Appendix A). This implies that the allowed fluctuations can be quite large, $|\varpi - k| \sim K^2/k$, so that the space–like, or time–like, nature of the current (depending upon the sign of $\varpi - k$) becomes apparent only for sufficiently large times, after the effects of the initial condition have dissipated. In fact, as we shall see in the next section, the early–time behavior of the solution $\psi(\tilde{t}, \chi)$ is independent of $K^2$, and hence the same for both space–like and time–like currents.

Another boundary condition refers to the behavior of the solution in the stationary regime (meaning, for large enough times) and at relatively large values of $\chi$ : since a black hole is a purely absorptive medium, from which no signal can escape, the solution $\psi(\tilde{t}, \chi)$ near the horizon located at $\chi = 2$ must be a purely outgoing wave (i.e., a wave departing from the boundary and impinging in the black hole). In fact, this outgoing–wave behavior should manifest itself already for relatively low values $\chi \ll 1$, and hence can be used as a boundary condition on Eq. (2.10), since the potential term in this effective Schrödinger equation is monotonous everywhere except near the boundary at $\chi = 0$, and hence it cannot generate reflected waves. This will be further discussed in the forthcoming sections.

## 3. Jets in the vacuum

We start with the zero–temperature case, i.e., with the propagation of the Abelian current through the vacuum. The results to be obtained here will not only serve as a level of comparison for the subsequent discussion of a plasma, but they will also prepare that discussion, at two levels (at least): First, as we shall see, there are special regimes (so like early times) where the dynamics in the plasma is quite similar to that in the vacuum. Second, the physical interpretation of our results, whose understanding is the main purpose in this paper, is easier to introduce and motivate in the context of the vacuum dynamics.

### 3.1 The vacuum polarization tensor

We begin this discussion with the *stationary case*, i.e., the case where the fields are purely plane waves in the physical, 4–dimensional, space, meaning that the fields denoted with a tilde in the previous discussion (e.g., $\tilde{A}_\mu$) are independent of time. The corresponding AdS/CFT calculation will provide the retarded current–current correlator (or 'polarization tensor') in Fourier space (with $q^\mu = (\omega, 0, 0, q)$) :

$$R_{\mu\nu}(q) \equiv i \int \mathrm{d}^4 x \, \mathrm{e}^{-iq\cdot x} \, \theta(x_0) \, \langle [J_\mu(x), J_\nu(0)] \rangle \, , \tag{3.1}$$

and in that sense it is the analog at strong coupling of computing momentum–space Fourier diagrams in perturbation theory at weak coupling. More precisely, $R_{\mu\nu}(q)$ is obtained by differentiating the classical action with respect to boundary values of the fields at $u = 0$ :

$$R_{\mu\nu}(q) = \frac{\partial^2 \mathcal{S}}{\partial A_\mu \partial A_\nu} \, , \tag{3.2}$$

where $A_\mu \equiv \tilde{A}_\mu(u = 0)$ in the notations of Eq. (2.2) and $\mathcal{S}$ is the four–dimensional action density, which is homogeneous: $S = \int \mathrm{d}^4 x \, \mathcal{S} = \Delta V \, \Delta t \, \mathcal{S}$, with $\Delta V \, \Delta t =$ the volume of space–time. In turn, the classical action density can be fully expressed (after using the equations of motion) in terms of the values of the field $\tilde{A}_\mu(u)$ and of its first derivative at $u = 0$ :

$$\mathcal{S} = \frac{N^2 T^2}{16} \left[ -\tilde{A}_0 \partial_u \tilde{A}_0^* + f \tilde{A}_3 \partial_u \tilde{A}_3^* + f \tilde{A}_i \partial_u \tilde{A}_i^* \right]_{u=0} \, , \tag{3.3}$$

where the $z$ component $\partial_u \tilde{A}_3$ is determined by the EOM as $\partial_u \tilde{A}_3 = -(\varpi/kf)\partial_u \tilde{A}_0$. A star on a field denotes complex conjugation: the classical solutions develop an imaginary part (in spite of obeying equations of motion with real coefficients) because of the outgoing–wave condition at large $u$ (see below). Via Eq. (3.2), this introduces an imaginary part in $R_{\mu\nu}(q)$ which physically describes the dissipation of the current in the original gauge theory. In fact, the imaginary part of the expression within the square brackets in Eq. (3.3) is independent of $u$ (as it can be checked by using the EOM) and hence it can be evaluated at any $u$ [25].

Note that, even in this zero–temperature context, we keep using the dimensionless variables $u$ and $\chi$, which were previously defined with respect to the black–hole horizon $r_0 = \pi R^2 T$. Throughout this section, it will be understood that $r_0$ and $T$ are arbitrary (length and, respectively, momentum) scales of reference, which are used to construct dimensionless coordinates at intermediate stages of the calculations, but which will drop out from the final, physical, results. In this context, the radial coordinates $u$ and $\chi$ can take on all the values from 0 to $\infty$.

We now turn to the actual calculation of the vacuum polarization tensor for the $\mathcal{N} = 4$ SYM theory in the strong coupling limit. The outcome of this calculation is already known (the case of a space–like current has been treated in detail in Ref. [9]), so our subsequent presentation will be very streamlined, with emphasis on the physical interpretation of the results. We shall give details for the longitudinal sector alone. The relevant equation reads (cf. Eq. (2.4) in which we let $f \to 1$ and $\partial^2/\partial \tilde{t}^2 \to -\varpi^2$)

$$a'' + \frac{1}{u} a' \mp \frac{K^2}{u} a = 0 \, , \tag{3.4}$$

where we recall that the upper (lower) sign in front of $K^2 \equiv |k^2 - \varpi^2|$ corresponds to a space–like (time–like) current. After the change of variable $\chi \equiv 2\sqrt{u}$, this is recognized as the equation for the $\nu = 0$ Bessel functions, of either real, or imaginary, argument (depending upon the sign in front of $K^2$). The solution is constrained by the boundary condition (see Ref. [9] for details)

$$\lim_{u \to 0} \left[ u a'(u) \right] = k(kA_0 + \varpi A_3)\big|_{u=0}, \qquad (3.5)$$

together with the condition of regularity at $u \to \infty$. For the space–like case, these conditions uniquely determine the solution as

$$a(u) = -2k(kA_0 + \varpi A_3)\big|_{u=0} K_0(2K\sqrt{u}) \qquad \text{(space–like)}. \qquad (3.6)$$

The other independent solution, $I_0(2K\sqrt{u})$, is rejected since it would exponentially diverge as $u \to \infty$. For the time–like case, on the other hand, the general solution is a superposition of oscillating Bessel functions,

$$a(u) = c_1 J_0(2K\sqrt{u}) + c_2 N_0(2K\sqrt{u}), \qquad (3.7)$$

so the condition of regularity at $u \to \infty$ introduces no constraint. To fix the solution in this case, we shall require $a(t, u) = e^{-i\omega t} a(u)$ to be an *outgoing wave* at large $u$; then, the solution becomes imaginary, with the appropriate sign for the imaginary part to yield the *retarded* polarization tensor, via Eq. (3.2). This constraint implies $c_1 = -ic_2$ which together with the boundary condition (3.5) completely fixes the solution as

$$a(u) = -i\pi k(kA_0 + \varpi A_3)\big|_{u=0} H_0^{(1)}(2K\sqrt{u}) \qquad \text{(time–like)}, \qquad (3.8)$$

where $H_0^{(1)} = J_0 + iN_0$ is a Hankel function encoding the desired outgoing–wave behavior at large $u$ : $a(t, u) \propto e^{-i(\omega t - K\chi)}$ when $\chi \equiv 2\sqrt{u} \gg 1/K$.

The transverse–wave solutions can be similarly obtained, but the above solutions for the longitudinal wave are in fact sufficient to complete the calculation of $R_{\mu\nu}(q)$: by Lorentz and gauge symmetry, the polarization tensor is transverse (with $\eta_{\mu\nu} = (-1, 1, 1, 1)$) :

$$R_{\mu\nu}(q) = \left( \eta_{\mu\nu} - \frac{q_\mu q_\nu}{Q^2} \right) R(Q^2) \qquad \text{(vacuum)}, \qquad (3.9)$$

and the scalar function $R(Q^2)$ can be computed with the longitudinal waves alone. A standard calculation, which involves the removal of a logarithmic divergence in the real part at $u = 0$ (the AdS/CFT analog of ultraviolet renormalization), finally yields

$$R(Q^2) = \frac{N_c^2 |Q^2|}{32\pi^2} \left( \ln \frac{|Q^2|}{\mu^2} - i\pi\Theta(-Q^2)\text{sgn}(\omega) \right), \qquad (3.10)$$

where $Q^2 \equiv -\omega^2 + q^2$ is the current virtuality in physical units and $\mu$ is the renormalization scale. As expected, the imaginary part is non–zero only for a time–like ($Q^2 < 0$) current, which can decay into the massless fields (adjoint scalars and Weyl fermions) of the $\mathcal{N} = 4$ SYM theory carrying $\mathcal{R}$–charge.

As anticipated in the Introduction, this result (3.10) is exactly the same as the respective perturbative result to one–loop order, so in particular its imaginary part (formally) describes the current decay into one pair of massless fields (a quark–antiquark pair, or two scalar fields). This interpretation is, of course, only formal: At strong coupling, the current can couple to arbitrarily complicated multi–particle states, but it so happens that, for the $\mathcal{N} = 4$ SYM theory, the total cross–section is determined by the two–particle final states alone. Our present calculation being an 'inclusive' one — it provides the total cross–section, but it does not discriminate between the various final states —, its result cannot give us any direct insight into the nature of these final states. We shall later try to gain such an insight based on physical considerations.

We conclude this discussion of the stationary case with another point of physical interpretation, which points towards an interesting 'duality' between the radial dimension in $AdS_5$ and the transverse size of the current (or, more precisely, of the partonic system into which the current has evolved) in the physical Minkowski space. Consider a space–like current, for definiteness. The modified Bessel function in Eq. (3.6) decays exponentially when $2K\sqrt{u} \gg 1$, meaning that the current penetrates in the radial dimension only up to a finite distance $u_0 \sim 1/4K^2$, or $\chi_0 \sim 1/K$ (recall that $\chi \equiv 2\sqrt{u}$). The more virtual the current is, the closer it remains to the boundary. This is quite similar to the picture of the current in transverse space, as familiar in perturbation theory (for either QCD or $\mathcal{N} = 4$ SYM): the virtual current fluctuates into a quark–antiquark pair (a 'color dipole') whose transverse size is inversely proportional to the current virtuality: $L \sim 2/Q$. This analogy is in fact even closer: the longitudinal wave solution in Eq. (3.6) involves the same modified Bessel function as the wavefunction describing the dipole fluctuation of a longitudinal photon in lowest order perturbation theory, which allows us to identify the respective arguments as $K\chi \leftrightarrow QL/2$. Recalling that $K = Q/2\pi T$ for a space–like current, we deduce the correspondence $\chi \leftrightarrow \pi TL$. The same argument holds in the transverse sector, where $K_0$ is replaced by $K_1$. Also, the argument can be adapted to a time–like current, since the oscillatory Bessel functions in Eq. (3.8) are rapidly decaying at radial distances $u \gg 1/4K^2$.

The above writing of the correspondence between the transverse size of the partonic fluctuation and the radial coordinate in $AdS_5$, namely, $\chi \leftrightarrow \pi TL$, explicitly involves the temperature and hence it might look a bit formal in the present context of the vacuum (but this writing will be natural for the subsequent discussion of a plasma). To avoid confusion, it is preferable to recall the definition $\chi \equiv 2(r_0/r)$ with $r_0 \equiv \pi R^2 T$ in order to rewrite this correspondence in the form $2R^2/r \leftrightarrow L$, from which the temperature has dropped out.

To summarize the previous discussion, the vacuum polarization tensor in the $\mathcal{N} = 4$ SYM theory at strong coupling formally describes the fluctuation of the current into a pair of elementary, massless, fields, whose transverse size appears to be in a one–to–one correspondence with the radial distance for the current penetration in $AdS_5$. As we shall see, this interpretation is comforted by the discussion of the time–dependent case, to which we now turn.

## 3.2 Jet evolution in the vacuum

As explained in Sect. 2, we are interested in the time evolution of vector fields $\tilde{A}_\mu(t, u)$ which at $t = 0$ start as a perturbation localized near $u = 0$ (or $\chi = 0$). Given the correspondence between $\chi$ and $L$ (the transverse size of the current), as argued at the end of the previous subsection, we

see that this initial condition corresponds to a current which, at $t = 0$, is point–like in transverse space. To describe its evolution, we shall use the Schrödinger form of the equations of motion, cf. Eqs. (2.9)–(2.10), and focus on the longitudinal sector, for definiteness. The vacuum version of these equations is obtained by removing the last term $\propto \chi^4$ in the potential; this yields, e.g.,

$$i\frac{\partial \psi}{\partial \tilde{t}} = \left( -\frac{1}{2k} \frac{\partial^2}{\partial \chi^2} - \frac{1}{8k\chi^2} \pm \frac{K^2}{2k} \right) \psi \,, \tag{3.11}$$

for which we shall construct solutions obeying the relevant initial and boundary conditions. To remain as simple as possible, we shall consider approximate solutions which are valid piece-wise in $\chi$ and which are sufficient to illustrate the main points of physics. A more systematic method to construct solutions to Eq. (3.11), which is based on the wave–packet decomposition in Eqs. (2.12)–(2.13), will be described in Appendix A.

We first note that at early times, so long as $\chi$ remains smaller than a critical value $\chi_c \simeq 1/2K$ (the corresponding limit on time will be determined later on), the second term, proportional to $K^2$, in the potential in Eq. (3.11) can be neglected compared to the first term $\propto 1/\chi^2$. Thus, this early–time dynamics is identical for both space–like and time–like currents. With the $K^2$ term omitted, Eq. (3.11) admits the following, exact, solution

$$\psi(\tilde{t}, \chi) = -i\frac{\sqrt{\chi}}{\tilde{t}} \, \mathrm{e}^{i\frac{k\chi^2}{2\tilde{t}}} \,. \tag{3.12}$$

This implies that the actual longitudinal wave (cf. Eq. (2.8))

$$\tilde{a}(\tilde{t}, \chi) = \frac{1}{\sqrt{\chi}} \psi \propto \frac{1}{\tilde{t}} \, \mathrm{e}^{i\frac{k\chi^2}{2\tilde{t}}} \,, \tag{3.13}$$

is localized near $\chi = 0$ at $\tilde{t} = 0$ (although this is not exactly a delta function). With increasing time, the energy density carried by the wave (3.13) diffuses towards larger values of $\chi$, so that the typical distance traveled by the corresponding wave–packet after a time $\tilde{t}$ is

$$\chi_{\mathrm{diff}}(\tilde{t}) \simeq \sqrt{\frac{2\tilde{t}}{k}} \,. \tag{3.14}$$

This behavior holds so long as $\chi_{\mathrm{diff}}(\tilde{t}) \lesssim 1/2K$, meaning for times $\tilde{t} \lesssim \tilde{t}_c \sim k/K^2$. In physical units, this yields $t_c \sim q/|Q^2|$, which is precisely the *coherence time* of the high–energy current; that is, this is the time interval which controls the Fourier transform[2] in Eq. (3.1), as it can be checked by rewriting the complex exponential there as

$$\mathrm{e}^{-i\omega t + iqz} \simeq \mathrm{e}^{-iq(t-z) + iQ^2 t/2q} \,, \tag{3.15}$$

where we have used $\omega \simeq q - Q^2/2q$ at high energy.

It is interesting to compare these results with the evolution of the quark–antiquark ('dipole') fluctuation of a virtual photon in perturbation theory in QCD: if the photon dissociates at $t = 0$

---

[2]At least in the vacuum, i.e., in the absence of other time scales which are introduced by a medium. As we shall see in Sect. 4, a finite–temperature plasma introduces a new such a scale indeed.

into a point–like pair of fermions, then with increasing time the transverse size of this pair is increasing diffusively, due to quantum dynamics, like [26, 27]

$$L \sim \sqrt{\frac{t}{q}}, \tag{3.16}$$

until it reaches a maximal size $L \sim 1/\sqrt{|Q^2|}$ at a time $t_c \sim q/|Q^2|$. (To avoid cumbersome notations, we shall often write $Q$ instead of $\sqrt{|Q^2|}$ and $Q^2$ instead of $|Q^2|$ within parametric estimates. For instance, the coherence time will be estimated as $t_c \sim q/Q^2$, where the modulus on $Q^2$ is implicit for a time–like current.) For $t > t_c$, the pair is either recombining back into a photon, or — if the photon was time–like — it splits apart, thus giving rise to two on–shell particles which move away from each other.

Clearly, the early time ($t < t_c$) evolution of the $q\bar{q}$ fluctuation in perturbation theory is very similar to the corresponding evolution of the vector perturbation in $AdS_5$ provided one identifies $\chi \sim TL$, in agreement with the discussion at the end of Sect. 3.1. As we show now, this correspondence persists also for larger times $t > t_c$.

Indeed, for $\tilde{t} \gg \tilde{t}_c$, one can heuristically estimate the time–derivative in the l.h.s. of Eq. (3.11) as $\partial/\partial\tilde{t} \ll 1/\tilde{t}_c \sim K^2/k$ (this heuristic argument will be confirmed by the wave–packet analysis in Appendix A). That is, the time–derivative term in the equation is much smaller than the last term $\sim K^2/k$ in the potential, which becomes the dominant term when $\chi \gg 1/2K$. Hence, for $\tilde{t} \gg \tilde{t}_c$ and $\chi \gg \chi_c$, the equation simplifies to

$$\frac{\partial^2}{\partial\chi^2}\psi = \pm K^2\psi, \tag{3.17}$$

(i.e., Schrödinger equation in a flat potential) with the obvious, acceptable, solutions

$$\psi(\chi) \propto \begin{cases} \mathrm{e}^{-K\chi} & \text{(space–like)} \\ \mathrm{e}^{iK\chi} & \text{(time–like)}. \end{cases} \tag{3.18}$$

which are time–independent and coincide, as they should, with the asymptotic versions (valid at large $\chi \gg 1/K$) of the respective stationary solutions constructed in Sect. 3.1. In the space–like case, the above solution confirms that, for times $t > t_c$, the perturbation remains localized near the boundary, within a distance $\chi \lesssim 1/K$. In the time–like case, it implies that the actual wave

$$a(\tilde{t}, \tilde{z}, \chi) = \mathrm{e}^{-i\varpi\tilde{t}+ik\tilde{z}} \frac{\psi}{\sqrt{\chi}} \propto \exp\left\{ -ik(\tilde{t}-\tilde{z}) - i\frac{K^2}{2k}\tilde{t} + iK\chi \right\} \tag{3.19}$$

propagates with constant group velocity $v_g = K/k \ll 1$ along the radial direction of $AdS_5$ :

$$\frac{\partial}{\partial K}\left(\frac{K^2}{2k}\tilde{t} - K\chi\right) = 0 \quad \implies \quad \chi_g(\tilde{t}) = \frac{K}{k}\tilde{t}. \tag{3.20}$$

Note that, for $\tilde{t} \sim \tilde{t}_c$, we have $\chi_g \sim 1/K$, as it should for consistency with the previous solution at early times. Hence, after the wave packet has diffused up to a distance $\chi_c \sim 1/K$ inside the bulk of $AdS_5$, it furthermore propagates with constant radial velocity, so like a free particle.

This free–motion pattern at $t > t_c$ looks, of course, natural, in view of the flatness of the potential in Eq. (3.17). In Appendix B, we shall verify that Eq. (3.20) is the same as the radial part of the geodesics of a massless classical particle which propagates in $AdS_5$ with longitudinal velocity $v_z = q/\omega$ and radial velocity $v_\chi = Q/\omega$, which is the same as the group velocity in Eq. (3.20) (recall that $\omega \simeq q$); this classical particle is massless since $v_z^2 + v_\chi^2 = 1$. On the other hand, the classical particle dynamics cannot reproduce the diffusion at early stages (a genuinely quantum effects), nor the fall of the wave into the black hole (to be later described, in Sect. 4.3).

Via the correspondence $\chi \leftrightarrow \pi T L$, the result in Eq. (3.20) is again consistent with the transverse dynamics expected for a time–like current which dissociates into a pair of massless particles (in lowest–order perturbation theory). Indeed, this result translates into

$$L(t) \simeq 2 \frac{\sqrt{\omega^2 - q^2}}{\omega} t = 2\sqrt{1 - v_z^2}\, t = 2\, v_\perp t\,, \tag{3.21}$$

where $v_z = q/\omega$ is the common longitudinal velocity of the two massless particles, as inherited from the current, and $v_\perp = \sqrt{1 - v_z^2}$ is the modulus of their transverse velocity: the two particles move in opposite directions in the transverse plane, so the transverse distance between them increases like $L = 2v_\perp t$. The above results have been obtained by working in the high–energy regime where $\omega \simeq q \gg Q$. However, it is easy to repeat the analysis for other regimes, with similar conclusions. For instance, for a zero–momentum current ($q = 0$, $Q = \omega$), one finds that $\chi_g(\tilde{t}) = \tilde{t}$, i.e., the two particles move in the transverse plane at the speed of light ($v_\perp = 1$).

At this point, one should again stress that the reason why the physical picture looks so simple in the strongly–coupled $\mathcal{N} = 4$ SYM theory is because of the non–renormalization property of the current–current correlator, as alluded to before. The AdS/CFT calculation correctly provides the total cross–section for the current decay, but it does not capture the detailed nature of the final states. Formally, the total cross–section is saturated by the two–particle final state; therefore, it is the dynamics of this particularly simple state which emerges, via the correspondence $\chi \leftrightarrow \pi T L$, from the dual calculation on the gravity side.

This discussion has an interesting corollary: it shows that the current can be also viewed as a device for introducing a pair of elementary, massless, fields of the $\mathcal{N} = 4$ SYM theory (Weyl fermions or adjoint scalars) at a given radial distance within $AdS_5$, which is controlled by the current virtuality: $\chi \sim 1/K$ or $r \sim QR^2$. This is tantamount to fixing the transverse size $L \sim 2/Q$ of the partonic pair in the physical space. That is, the dynamics of the current at times larger than the coherence time is the same as that of 'meson', or of a 'color dipole'. For a space–like current, this effective 'meson' simply sits at $\chi \sim 1/K$, meaning that its transverse size is fixed. For a time–like current, this 'meson' propagates with constant velocity along the radial direction $\chi$, meaning that its transverse size grows at constant speed. In the next section we shall study the influence of a thermal bath on this dynamics.

## 4. Jets in the plasma

We now turn to the problem of main interest for us here, which is the propagation of the current and of the associated partonic system through a strongly–coupled $\mathcal{N} = 4$ SYM plasma with

temperature $T$. We are interested in 'hard probes', so we shall choose a current with relatively high virtuality (either space–like, or time–like) : $Q \equiv \sqrt{|Q^2|} \gg T$ (or $K \gg 1$), which probes the structure of the plasma on distances much shorter than the thermal wavelength $1/T$. We shall mostly consider a relativistic current, for which $q \simeq \omega \gg Q$, but the non–relativistic case ($q \ll \omega$) will be briefly discussed too, for completeness. In fact, the physically most interesting case — the one where the medium effects should be truly relevant — is when the coherence time $t_c \sim q/Q^2$ of the current is much larger than $1/T$, so that the current explores a relatively large longitudinal slice of the plasma, with width $\Delta z \sim t_c \gg 1/T$. This implies a lower limit on the current momentum: $q \gg Q^2/T$, which is tantamount to the condition that the Bjorken–$x$ variable[3], defined as $x \equiv Q^2/2qT$ (in the plasma rest frame), be very small: $x \ll 1$.

## 4.1 Physical regimes

We would like to determine the characteristic time scale for the dissipation of the current in the plasma; in the dual, gravity, problem, this is the time scale for the fall–off of the Maxwell field $A_\mu$ into the black hole. As we shall see, this scale is controlled by the dynamics at relatively small $u \ll 1$, and thus is insensitive to the detailed geometry of the black hole near its horizon at $u = 1$. As explained in Sect. 2, the strength of the gravitational interactions between the wave and the black hole is proportional to the wave longitudinal momentum $q$, and also to the temperature. In view of that, we shall be led to distinguish between two important physical regimes:

(i) a relatively low–energy (or low–temperature) regime at $qT^2 \ll Q^3$ (or $k \ll K^3$), where the medium effects are strongly delayed, so that the current dynamics proceeds as in the vacuum up to time scales much larger than $t_c$, and

(ii) a very high–energy (or high–temperature) regime at $qT^2 \gg Q^3$ (or $k \gg K^3$), in which the current dissipates very fast, on a time scale much shorter than $t_c$.

One can understand these various regimes by studying the potential in the Schrödinger–like equations (2.9)–(2.10). Let us first recall from the previous section that the time–dependence in these equations is important only at very early stages, when the typical values of $\chi$ are so small that the only relevant term in the potential is the first term, $\propto 1/k\chi^2$, which is independent of both the current virtuality and the properties of the medium. Hence, for such early times, the equations describe diffusion, for both space–like and time–like currents, and in the same way as in the vacuum. But for later times, where the meaning of 'later' is generally medium– and energy–dependent (see below), the solutions approach a stationary regime, where Eqs. (2.9)–(2.10) can be replaced by their time–independent versions, of the generic form $-\psi'' + V\psi = E\psi$ with $E = 0$ (since $E$ corresponds to the time–derivative, which is negligible). Hence, this late–time behavior is determined by the time–independent Schrödinger solution with zero energy in the potential $V(\chi)$.

In what follows we shall study this solution in the longitudinal sector alone (the corresponding discussion for the transverse sector being very similar). The respective potential is graphically illustrated in Figs. 1, 2, and 3, for the various physical regimes: low energy and

---

[3]This variable is especially relevant for a space–like current which undergoes deep inelastic scattering off the plasma [9].
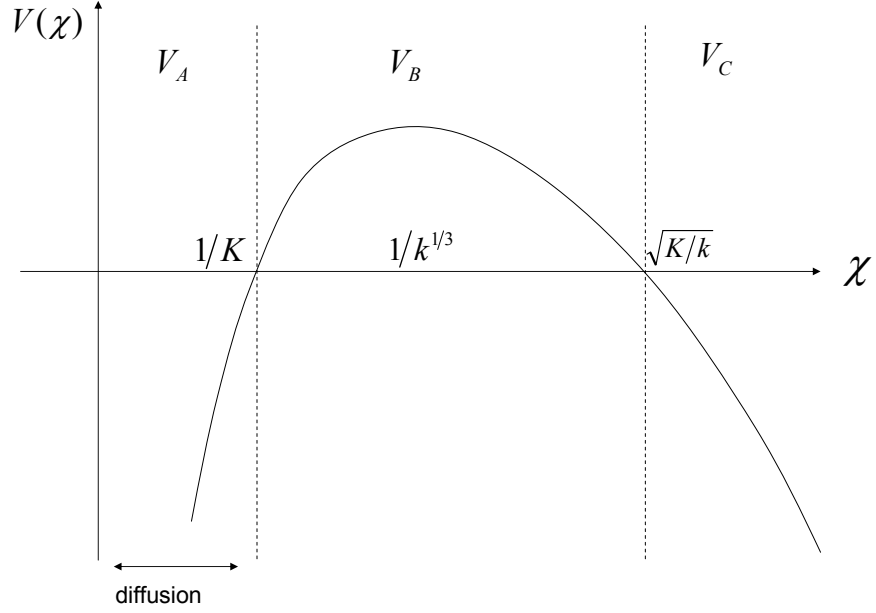
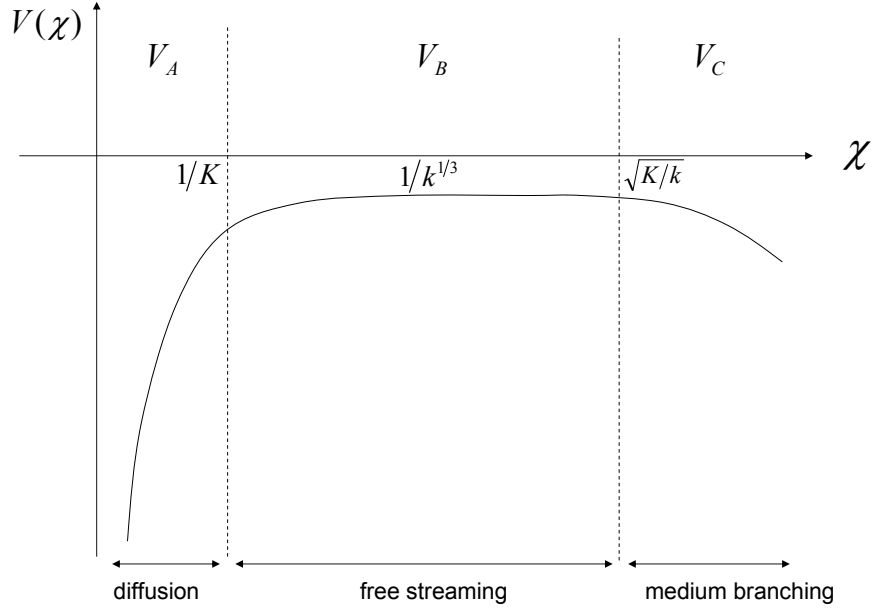**Figure 1:** *The potential in Eq. (2.10) for the space–like case at relatively low energy ($k \ll K^3$).*



**Figure 2:** *The potential in Eq. (2.10) for the time–like case at relatively low energy ($k \ll K^3$).*

space–like in Fig. 1, low energy and time–like in Fig. 2, and high energy (both space–like and time–like) in Fig. 3. Some general features of the dynamics are already clear by inspection of these figures: At sufficiently small values of $\chi$, the potential is the same as in the vacuum; the medium starts to be felt only at relatively large values of $\chi$, where the potential is a decreasing function which describes attraction by the black hole. Also, in the high–energy regime, the dynamics is essentially the same for both space–like and time–like currents. Finally, in the space–like case at least, there is an obvious difference between the low–energy regime, where
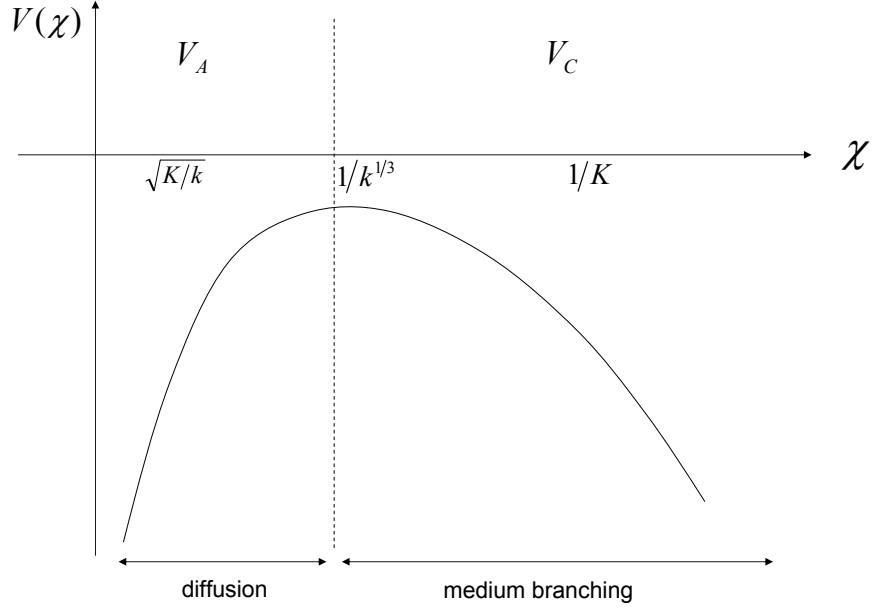
– 16 –

**Figure 3:** *The potential in Eq. (2.10) in the high–energy regime at $k \gg K^3$, where this potential is essentially the same for both space–like and time–like currents.*

the potential barrier constrains the wave to remain on the left of the 'classical turning point' at $\chi \sim 1/K$ (so like in the vacuum), and the high–energy regime, where the barrier has disappeared and the wave can easily propagate towards the horizon. (The transition between the two regimes occurring at $k \sim K^3$ corresponds precisely to the situation where the height of the potential barrier becomes negligible.) In the time–like case, on the other hand, there is never such a barrier, so the difference between the low–energy and high–energy regimes looks perhaps less obvious. As we now explain, this difference is nevertheless important in that case too.

To that aim, it is convenient to separate the three pieces in the potential in Eq. (2.10), which play different physical roles. We thus write (for a time–like current)

$$V(\chi) = -\frac{1}{8k\chi^2} - \frac{K^2}{2k} - \frac{k\chi^4}{32} \equiv V_A + V_B + V_C. \tag{4.1}$$

Let $\chi_{AB}$ denote the value of $\chi$ at which $V_A$ and $V_B$ become comparable with each other, and similarly for $\chi_{AC}$ and $\chi_{BC}$. We have, parametrically,

$$\chi_{AB} \sim \frac{1}{K}, \qquad \chi_{AC} \sim \frac{1}{k^{1/3}}, \qquad \chi_{BC} \sim \sqrt{\frac{K}{k}}. \tag{4.2}$$

Consider now the two physical regimes alluded to before:

(i) Low energy regime : $k \ll K^3 \implies \chi_{AB} \ll \chi_{AC} \ll \chi_{BC}$

It is easy to check that, in this regime, the potential admits the piecewise approximation

$$V(\chi) \propto \begin{cases} V_A + V_B & \text{for } \chi \ll \chi_{BC} \\ V_C & \text{for } \chi \gg \chi_{BC}. \end{cases} \tag{4.3}$$

Thus, so long as the relevant values of $\chi$ (those where most of the wave energy is located) remain much smaller than $\chi_{BC}$, the dynamics is the same as in the vacuum. This is the situation at sufficiently small times, that we shall study in the next subsection. But when $\chi \gtrsim \chi_{BC}$, the medium effects become important and entail the fall of the wave into the black hole. This fall be studied in Sect. 4.3. Note that the transition point $\chi \sim \chi_{BC}$ is where the potential changes from a plateau to a rapidly decreasing function (see Fig. 2).

(ii) High energy regime : $k \gg K^3 \implies \chi_{BC} \ll \chi_{AC} \ll \chi_{AB}$

In this regime, the virtuality–dependent piece $V_B$ is never important, and the potential can be approximated as (see also Fig. 3)

$$V(\chi) \propto \begin{cases} V_A & \text{for } \chi \ll \chi_{AC} \\ V_C & \text{for } \chi \gg \chi_{AC}, \end{cases} \tag{4.4}$$

which now holds for both space–like and time–like currents. Unlike the low–energy potential, the high–energy one has no intermediate plateau, but only a pronounced peak at $\chi \sim \chi_{AC}$. In fact, the transition between the two energy regimes, which occurs for $k \sim K^3$, corresponds to the situation where the two endpoints of the plateau, $\chi_{AB}$ and $\chi_{BC}$, merge with each other, and also with the position $\chi_{AC}$ of the emerging peak.

## 4.2 Early–time dynamics

In this subsection, we shall consider the dynamics of the current at early times, which is insensitive to medium effects (except for its validity limits, as introduced by the plasma), and thus can be inferred from the corresponding discussion in Sect. 3.

We start with a simple case, which has not been explicitly covered by the previous discussion, but which can be viewed as a special limit of the low–energy case: a non–relativistic, time–like, current with $q \ll \omega$ and $\omega \gg T$. The corresponding 'Schrödinger' equations are obtained from Eqs. (2.9)–(2.10) by omitting the last, medium–dependent, term in the potential (since this term is comparatively small for any $0 \leq \chi \leq 2$) and replacing $k \to \varpi$ and $K^2 \to \varpi^2$ in all the other terms. The ensuing equations are the same as in the vacuum, and therefore so is also the current dynamics, until it eventually dissipates into the plasma. Specifically, at very early times $\tilde{t} \lesssim 1/\varpi$, the associated Maxwell wave diffusively penetrates into $AdS_5$, up to a distance $\chi \sim 1/\varpi$ (meaning that the current diffusively spreads out in the physical space, up to a size $L \sim 1/\omega$). Then, for larger times $\tilde{t} \gg 1/\varpi$, the wave propagates inside $AdS_5$ with constant group velocity $v_g = 1$, meaning that the current has decayed into a pair of massless particles which move away from each other at the speed of light: $\chi_g(\tilde{t}) = \tilde{t}$, or $L(t) = 2t$. This behavior continues until the wave hits the horizon ($\chi_g = 2$ or $\tilde{t} \sim 1$) and is thus absorbed by the black hole. Physically, this means that, for times $t \sim 1/T$, the separation between the products of the current decay has become as large as the thermal wavelength, $L \sim 1/T$, so these products cannot be anymore distinguished from the plasma fluctuations — they get 'lost' in the plasma.

We now turn to a relativistic current with $\varpi \sim k \gg K^2$, for which we have to distinguish between two physical regimes, as previously explained:

(i) At moderate energies, such that $K^2 \ll k \ll K^3$, and for a time–like current, the upper limit $\chi_{BC} \sim \sqrt{K/k}$ for the vacuum–like behavior is much larger than $\chi_{AB} \sim 1/K$, which is

the maximal penetration length through diffusion. Hence, in this regime, one can observe both stages of the evolution identified in Sect. 3: a 'diffusive' stage at early times $\tilde{t} \lesssim \tilde{t}_c \sim k/K^2$, during which the wave–packet progresses according to Eq. (3.14), and a 'free motion' stage at $\tilde{t} > \tilde{t}_c$, during which the wave has constant group velocity $v_g = K/k$. This second stage lasts until the position $\chi_g(\tilde{t}) = v_g \tilde{t}$ of the wave–packet becomes comparable to $\chi_{BC}$; this happens at a time $\tilde{t}_f \sim \sqrt{k/K}$ (the subscript $f$ on $\tilde{t}_f$ stands for "free motion"), which represents the upper time limit for this vacuum–like dynamics. In physical units, this yields a time scale

$$t_f \sim \frac{1}{T} \sqrt{\frac{q}{Q}} \gg t_c \sim \frac{q}{Q^2} \gg \frac{1}{T}, \tag{4.5}$$

which, as indicated above, is much larger than the coherence time.

The physical interpretation of this result, as deduced via the correspondence $\chi \leftrightarrow \pi T L$, is as follows: the time–like current develops a partonic fluctuation with size $L \sim 1/Q$ over a time of the order of the coherence time $t_c$, and then decays into a system of massless particles which move freely (without feeling the plasma) up to a time $t \sim t_f$. At this stage, the transverse extent of the partonic system has increased up to a value

$$L_f = 2v_\perp t_f \sim \frac{1}{T} \sqrt{\frac{Q}{q}} \ll \frac{1}{T}, \tag{4.6}$$

which is still small as compared to the thermal wavelength in the medium. For even later times $t > t_f$, the dynamics is driven by the medium and will be analyzed in the next subsection.

It is interesting to notice at this point that, although it influences the dynamics at late times $t > t_f$, the plasma has no effect on the polarization tensor, which is still given by the same expression as in the vacuum, namely Eqs. (3.9)–(3.10) with $Q^2 < 0$. Indeed, if one considers a (time–like) plane–wave solution, so like in Sect. 3.1, then for $\chi \ll \chi_{BC}$ this solution is again given by Eq. (3.8), which describes an outgoing wave for any $\chi$ within the range $\chi_{AB} \ll \chi \ll \chi_{BC}$. The change in the solution at larger $\chi \gtrsim \chi_{BC}$ has no incidence on the calculation of $R_{\mu\nu}(q)$, which is determined by the behavior of the solution near $\chi = 0$, cf. Eq. (3.2). Physically, this is so since the current disappears by decaying into a pair of massless fields, so like in the vacuum, and the subsequent fate of these fields is irrelevant for the calculation of the total decay rate (the imaginary part of $R_{\mu\nu}$). This is similar to the calculation of the total cross–section for $e^+e^-$ annihilation in lowest–order perturbation theory: this cross–section is fully given by the $e^+e^-$ annihilation into a $q\bar{q}$ pair, although the quark and the antiquark are not the actual final states in the experiments. The 'late stages' radiations or interactions involving the quark and the antiquark, although essential for hadronisation and the composition of the final state, do not affect the total $e^+e^-$ cross–section.

(ii) At ultrarelativistic energies $k \gg K^3$, the medium effects (as enhanced by the energy) become important already at the very short radial distance $\chi_{AC} \sim 1/k^{1/3} \ll 1/K$, meaning that the current has no time to fully develop its partonic fluctuation before getting absorbed. At very early times, such a fluctuation starts to develop via diffusion, but this process is interrupted after the relatively short period $\tilde{t}_s \sim k^{1/3}$, or

$$t_s \sim \frac{1}{T} \left(\frac{q}{T}\right)^{1/3} \ll t_c \sim \frac{q}{Q^2}, \tag{4.7}$$

(which is still bigger than $1/T$ though), when the wave–packet has diffused up to $\chi_{AC}$. Physically, this means that the growth of the fluctuation is stopped at a transverse size

$$
L_s \sim \sqrt{\frac{t_s}{q}} \sim \frac{1}{T}\left(\frac{T}{q}\right)^{1/3} \ll \frac{1}{Q},
\tag{4.8}
$$

which is much smaller than the natural size $\sim 1/Q$ for the same fluctuation in the vacuum. Accordingly, the dynamics is very different from the vacuum case, in the sense that the dissipation of the current and the respective polarization tensor are now controlled by the medium. This polarization tensor, which is now identical for space–like and time–like currents, has been computed in Ref. [9], and the result was used to deduce a partonic interpretation for the structure of the plasma in its infinite momentum frame. In the next subsection, we shall address this problem from a different perspective, by following the time evolution of the Maxwell wave during its fall towards the black hole. The insight that we shall gain in this way will allow us to propose, in Sect. 5, a physical picture for the current dissipation in the strongly coupled plasma.

### 4.3 The fall of the wave into the black hole

We now come to the most interesting physical situation, which refers to the (relatively) late stages of the current evolution in the plasma and the mechanism for current dissipation. In this situation, the dynamics is controlled by the medium–dependent piece in the potential (the piece $V_c \sim \chi^4$ in Eq. (4.1)), which yields the following equation of motion in Schrödinger form

$$
i\frac{\partial \psi}{\partial \tilde{t}} = \left(-\frac{1}{2k}\frac{\partial^2}{\partial \chi^2} - \frac{k\chi^4}{32}\right)\psi\,.
\tag{4.9}
$$

As previously explained, for a time–like current this equation holds both at moderate energies, $K^2 \ll k \ll K^3$, and in the high–energy limit $k \gg K^3$, but in ranges for $\chi$ which are different in the two cases (cf. Eqs. (4.3)–(4.4)). For a space–like current, it holds only for $k \gg K^3$ and $\chi \gg \chi_{AC}$.

    We have not been able to find an exact solution to this equation, but we shall construct a WKB approximation to it. To that aim, we use the wave–packet representation in Eq. (2.12). The corresponding WKB solution reads then

$$
\psi(\tilde{t},\chi) = \int d\varepsilon\, e^{-i\varepsilon(\tilde{t}-\tilde{t}_0)-\frac{\varepsilon^2}{2\sigma^2}}\, \frac{1}{p_\varepsilon(\chi)}\, \exp\left\{i\int_{\chi_0}^{\chi} d\chi'\, p_\varepsilon(\chi')\right\},
$$

$$
p_\varepsilon(\chi) \equiv \sqrt{2k(\varepsilon - V_C(\chi))}\,,
\tag{4.10}
$$

where we have kept only the outgoing wave and $\chi_0$ is either $\chi_{BC}$, or $\chi_{AC}$, depending upon the physical regime under consideration (and similarly for $\tilde{t}_0$). At this point, we notice that the interesting values of $\tilde{t}$ are large enough for the typical energy $\varepsilon \sim 1/\tilde{t}$ to be much smaller than the potential $|V_C| \sim k\chi^4$. For instance, when $k \gg K^3$, we are interested in $\tilde{t} \gtrsim \tilde{t}_s \sim k^{1/3}$ together with $\chi \gg \chi_{AC} \sim 1/k^{1/3}$. Then we can expand the square root within $p_\varepsilon$ to linear order in $\varepsilon$ and perform the ensuing Gaussian integration, to obtain

$$
\psi(\tilde{t},\chi) \simeq \frac{1}{p_0(\chi)}\, \exp\left\{i\int_{\chi_0}^{\chi} d\chi'\, p_0(\chi') - \frac{\sigma^2}{2}\left[(\tilde{t}-\tilde{t}_0) - 4\left(\frac{1}{\chi_0} - \frac{1}{\chi}\right)\right]^2\right\}.
\tag{4.11}
$$

We have also used here

$$\left.\frac{\partial p_\varepsilon}{\partial \varepsilon}\right|_{\varepsilon=0} = \sqrt{\frac{k}{2|V_C|}} = \frac{4}{\chi^2} \implies \int_{\chi_0}^{\chi} d\chi' \left.\frac{\partial p_\varepsilon}{\partial \varepsilon}\right|_{\varepsilon=0} = 4\left(\frac{1}{\chi_0} - \frac{1}{\chi}\right). \tag{4.12}$$

The modulus $|\psi(\tilde{t},\chi)|$ tells us where the energy of the wave–packet is located at time $\tilde{t}$. Clearly, with increasing time, the peak of the energy distribution moves along a trajectory

$$\chi(\tilde{t}) = \frac{\chi_0}{1 - \frac{\chi_0}{4}(\tilde{t} - \tilde{t}_0)}, \tag{4.13}$$

which can be recognized as the trajectory of a classical particle with mass $m = k$ and zero total energy moving in the potential $V_C(\chi)$. This is so almost by construction (because the classical trajectory defines the group velocity for the WKB solution), and can be also checked by starting with the respective particle equation of motion, that is,

$$k \frac{d^2\chi}{d\tilde{t}^2} = -\frac{dV_c}{d\chi} = k\frac{\chi^3}{8}, \tag{4.14}$$

whose zero–energy solution brings us back to Eq. (4.13), as it should.

The approximation (4.13) holds only so long as $\chi \ll 1$, but it can be used to estimate the duration of the fall of the wave–packet in the potential; namely, $\chi(\tilde{t})$ reaches the horizon at $\chi = 2$ when $\tilde{t} \sim \tilde{t}_h$, with

$$\tilde{t}_h - \tilde{t}_0 = \frac{4}{\chi_0} - 2 \simeq \frac{4}{\chi_0}. \tag{4.15}$$

Note that, parametrically, $\chi_0 \sim 1/\tilde{t}_0$ for both the intermediate–energy and the high–energy regimes. Thus, $\tilde{t}_h - \tilde{t}_0 \sim \tilde{t}_0$, so the total time $\tilde{t}_h$ necessary for the wave–packet to propagate within $AdS_5$ from the boundary to the horizon is of order $\tilde{t}_0$. Essentially, half of this time is used to (rather slowly) reach the ' point of no return' at $\chi_0 \ll 1$ (the point where the wave starts to feel the attraction of the black hole) and the other half to travel along the considerably larger distance from $\chi_0$ up to the horizon. Clearly, for $\chi > \chi_0$ the motion of the wave–packet is accelerated by the gravitational force. In fact, Eq. (4.14) implies that the group velocity $\dot{\chi} \equiv d\chi/d\tilde{t}$ approaches the speed of light (from below) when the wave gets close to the horizon:

$$\dot{\chi} = \frac{\chi^2}{4} \implies \dot{\chi} \simeq 1 \quad \text{when} \quad \chi \simeq 2. \tag{4.16}$$

In reality, the particle cannot cross the horizon (in the laboratory frame), but only asymptotically approach to it, so its velocity can never become exactly one. But when $\chi \simeq 2$, the terms in the potential which have been neglected in writing Eq. (4.9) become important and modify Eq. (4.16). Let us also note here the 'dual' version of the above equation, which is particularly suggestive : using the correspondence $\chi \sim TL$ and introducing the parton transverse momentum $p_\perp$ via the uncertainty principle, i.e., $p_\perp \sim 1/L$, we arrive at

$$\frac{dp_\perp}{dt} \sim -T^2. \tag{4.17}$$

That is, there is a transverse force acting on the colored partons in the plasma, and this force is independent of the parton momentum and of order $T^2$. This result will play an important role in the physical discussion in Sect. 5.2.

Let us conclude this section with a brief summary of the previous results, in physical terms:

(i) At *moderately high energies*, such that $Q/T \ll q/Q \ll (Q/T)^2$, a time–like current creates SYM quanta in the plasma at $t = 0$, which then pass through three stages before disappearing :

(a) a relatively short period of *diffusion*, at $t \lesssim t_c$ with $t_c \sim q/Q^2$, during which the current gets replaced by a bunch of on–shell massless partons (only two such partons being manifest in our calculation), with overall transverse size $L \sim 1/Q$ ;

(b) a longer period of *free streaming*, from $t \sim t_c$ up to $t_f \sim (1/T)\sqrt{q/Q}$, during which the partonic system propagates without feeling the plasma and expands in transverse space up to a size $L \sim (1/T)\sqrt{Q/q} \ll 1/T$, and

(c) an equally long period, during which the interactions with the plasma cause an *accelerated expansion* in transverse space, up to a maximal size $L \sim 1/T$; when this size is reached, the partons move apart from each other at the speed of light ($v_\perp \simeq 1$) and disappear in the plasma.

The lifetime of the current is controlled by the two last stages, and thus is of order $t_f$, which is much larger than the coherence time $t_c$.

(ii) At *very high energies*, such that $q/Q \gg (Q/T)^2$, a virtual current, either time–like or space–like, goes through only two stages before dissipation:

(a) a relatively short period of *diffusion*, at $t \lesssim t_s$ with $t_s \sim q/Q_s^2(q) \ll t_c$, during which the partonic fluctuation coming from the current grows up to a transverse size $L \sim 1/Q_s(q)$, which is however not sufficient for the partons to become on–shell, and

(b) an equally short period of *accelerated expansion*, at times $t > t_s$, which lasts until the partonic fluctuation reaches a transverse size $L \sim 1/T$ and disappears in the plasma.

Both stages contribute on equal footing to the lifetime of the current, so this lifetime is of order $t_s$.

Above, we have introduced the *saturation momentum $Q_s(q) \sim (qT^2)^{1/3}$*, which is the natural transverse momentum scale to discuss the high–energy scattering off the plasma [9]. This is defined as the 'critical' virtuality for the transition between the low–energy and the high–energy regimes: we have indeed $q/T \sim (Q_s(q)/T)^3$. Note that, at high energy, $Q_s(q)$ replaces $Q$ as the virtuality scale which determines all the physically relevant scales for transverse size and time. (For instance, both $t_c$ and $t_f$ reduce to $t_s$ after the replacement $Q \to Q_s(q)$.) Moreover, $Q_s(q)$ is also the critical scale for the disappearance of the potential barrier in the space–like case.

## 5. Physical discussion

This section will contain no new technical developments, but in spite of that it could be viewed as the main section of this paper; indeed, here is where, on the basis of the previous results, we shall develop our physical picture. But before we do so, it is useful to make contact with some previous approaches in the literature. This should make clear that the physical picture that we shall later develop will also shed light on some of the results of these previous approaches.

## 5.1 Relation with previous approaches

In this subsection, we shall show that our previous results are consistent with, and shed new light on, previous studies in the literature [10, 11, 12, 13, 14, 15, 16, 17, 18], concerning the propagation of 'heavy quarks', or of quark–antiquark 'mesons', in the strongly coupled $\mathcal{N} = 4$ SYM plasma.

To be specific, let us start with an example (we shall present some others later on): Consider a time–like current at moderately high energy ($Q/T \ll q/Q \ll (Q/T)^2$) and focus on our estimate (4.6) for $L_f$ — the transverse size at which the partonic system created via the decay of the current starts to lose energy in the plasma. After introducing $v_z = q/\omega$ and $\gamma \equiv 1/\sqrt{1 - v_z^2} = q/Q$, this result can be rewritten as

$$L_f \sim \frac{1}{\gamma^{1/2}T} \quad \sim \quad \frac{(1 - v_z^2)^{1/4}}{T}, \tag{5.1}$$

which turns out to be the same as the parametric estimate for the 'meson screening length' $\ell_{\max}(v_z, T)$ computed in Refs. [10, 11, 12]. The latter is the maximal transverse size that a 'heavy meson' (a bound system of a quark and an antiquark) can have in the plasma, when it propagates along the $z$ axis with a constant velocity $v_z < 1$. So long as the transverse size $\ell$ of the meson is smaller than $\ell_{\max}(v_z, T)$, the $q\bar{q}$ pair is bound indeed and it moves freely through the plasma — that is, it moves at constant speed $v_z$ without the need for an external force. Mathematically, this is described by a string connecting the quark and the antiquark through $AdS_5$, which rigidly moves together with its endpoints. For $\ell > \ell_{\max}(v_z, T)$, on the other hand, this connecting–string solution ceases to exist and is replaced by two disjoint strings trailing behind the quark and, respectively, the antiquark, which extends in $AdS_5$ all the way up the horizon. This trailing strings exerce a drag force on their fermionic sources, meaning that energy is transferred from the quark and the antiquark to the black hole [17, 18, 28, 29].

This meson dynamics is similar to that emerging from the present calculation, except for the fact that, here, the transverse size of the partonic pair is not a free parameter any longer, but is rather fixed by the dynamics (and hence it depends upon time). Namely, over the time interval $t_c < t < t_f$, which is large as compared to the formation time $t_c \sim q/Q^2$ of the pair, the time–like current can be effectively viewed as a 'meson' made with a pair of on–shell, massless, partons (Weyl fermions or adjoint scalars), which propagate together along the $z$ axis with constant velocity $v_z$ and at the same time separate from each other in transverse directions with a (small) relative velocity $2v_\perp$, with $v_\perp = \sqrt{1 - v_z^2} \ll 1$. Hence, the transverse size of the 'meson' increases like $L = 2v_\perp t$. When this size reaches the critical value in Eq. (4.6) or (5.1) (this happens at a time $t \sim t_f \simeq \sqrt{\gamma}/T$), the partons start to lose energy to the plasma and then the 'meson' disappears, so like in the corresponding calculation in Refs. [10, 11, 12].

If this analogy is correct, then we should also find some similarity between the trailing–string solutions in Refs. [17, 18, 28, 29] and the dynamics of the current at *late* times $t \gg t_f$, where dissipation is important. We will later show that this is indeed the case, but before that let us emphasize some differences between our actual problem and those in the previous literature:

• Our 'partons' are massless fields from the Lagrangian of the $\mathcal{N} = 4$ SYM theory. A pair of such fields is produced by the current, at a distance $\chi \sim 1/K$ inside $AdS_5$ which is controlled by the current virtuality. Physically, this means that this pair is produced with a transverse

size $L \sim 1/Q$. By contrast, in previous studies, the 'partons' are 'heavy quark probes', that is, massive fermions which do not belong to $\mathcal{N} = 4$ SYM and whose introduction requires an extension of the original AdS/CFT correspondence: the dual partners of these fermions are open strings ending on a D7 brane which extends along the radial direction of $AdS_5$ up to a distance $\chi$ inversely proportional to the fermion mass. This makes it difficult to consider massless, or even light, quarks, since the corresponding D7 brane would enter the black hole. Moreover, difficulties appear even for heavy quarks in the high–energy limit ($v_z \to 1$), since the latter appears not to commute with the limit in which the ultraviolet cutoff is sent to infinity [19, 30, 15, 31]. This particular problem does not appear in our formalism, where physics is completely smooth in the limit $v_z \to 1$, even in crossing the lightcone.

• The partonic pair produced by the decay of a time–like current is, strictly speaking, not a 'meson' (i.e., a bound state which would be stable in the absence of the plasma), but rather a pair of jets, similar to the $q\bar{q}$ jets created via $e^+e^-$ annihilation in perturbative QCD. However, the relative velocity of these jets in transverse space is much smaller than their common longitudinal velocity ($v_\perp = \sqrt{1 - v_z^2} \ll v_z$), so the fields remain close to each other for a long time $\sim \sqrt{\gamma}/T$; this may explain why their dynamics is so similar to that of a meson. As we shall shortly argue, the partonic fluctuation of a *space–like* (relativistic) current is even closer to an actual meson.

• In our approach, there is no explicit string dual counterpart of the 'partons', or 'jets' (so like the endpoints of the string on the D7 brane in the 'meson' problem). The partons appear only in the physical interpretation on the gauge theory side, where they are supposed to be generated via current fluctuations. Related to that, the 't Hooft coupling $\lambda$, which in the other approaches is introduced by the Nambu–Goto string action, is not present in our formalism, which in fact corresponds to the strict strong–coupling limit $\lambda \to \infty$. This feature sometimes complicates the comparison between our results and previous approaches.

In spite of such differences, striking similarities persist (like the one already discussed in relation with Eq. (5.1)), which support the idea that the two types of problems (the 'current' and the 'meson') are closely related. In what follows, we shall give some more examples in that sense, which suggest that our wave–packet propagating through $AdS_5$ — the gravity dual of the plasma perturbation by a current — is in fact rather similar to the string solutions describing a meson, or heavy quark, perturbation in the previous approaches.

Consider first a time–like current at moderate energies and not so late times ($t < t_f$), corresponding to a relatively small meson. The dynamics of the connecting–string solution on the 'meson' side is characterized by two important scales in $AdS_5$ (see, e.g., [12, 15]) : the position $\chi_{\rm tip}(\ell)$ of the peak of the string (the maximal penetration of the string in $AdS_5$) and the radial coordinate $\chi_v = 2/\sqrt{\gamma}$ beyond which the string action would become imaginary. For a relatively small meson $\ell \ll \ell_{\rm max}(v_z, T)$, one finds $\chi_{\rm tip}(\ell) \sim T\ell$, which is precisely the relation between the distance traveled in $AdS_5$ and the transverse size of the partonic system that we advocated at the end of Sect. 3.2. This suggests that one can identify $\chi_{\rm tip}(\ell)$ with the position of our wave–packet in $AdS_5$. Furthermore, recalling that $\gamma = q/Q$, one sees that $\chi_v \sim \sqrt{Q/q}$ is the same as our 'point of no return' $\chi_{BC}$, cf. Eqs. (4.2) and (4.3) : beyond this point, the wave cannot escape the attraction by the black hole.

Similar identifications can be made also for a *space–like* current with moderate energy ($q \ll Q^3/T^2$): Then, $\chi_{\rm tip}(\ell)$ and $\chi_v$ correspond to the first and, respectively, second 'classical turning

points' for the potential barrier in Fig. 1, i.e., $\chi_{AB} \sim T/Q$ and, respectively, $\chi_{BC} \sim \sqrt{Q/q}$. The partonic system has now a fixed size $L \sim 1/Q$ (since the Maxwell wave gets stuck at $\chi \lesssim \chi_{AB}$), and in that sense it looks even closer to a real meson.

Returning to the case of a moderate–energy *time–like* current, let us now consider the dynamics at later times, $t \gtrsim t_f$, where we would like to make contact with the trailing–string solution in Refs. [17, 18]. Notice first that the criterion for the onset of dissipation, which determines the 'critical' length (5.1), is the same in our problem and in the 'meson' problem: this is the condition that the distance traveled in $AdS_5$ get close to the 'point of no return', which amounts to $\chi_g \sim \chi_{BC}$ (cf. the discussion above Eq. (4.5)) in our context, and to $\chi_{\rm tip} \sim \chi_v$ in the approach of Refs. [10, 11, 12]. There is an interesting difference though: whereas in the usual meson problem, this change of regime is abrupt and characterized by a sharp critical value $\ell_{\max}(v_z, T)$, in our approach it is much more gradual[4], as it is driven by the competition between the various terms in the potential. For $\chi \gg \chi_{BC}$ (and hence $t \gg t_f$), our solution describes a wave–packet falling into the black hole, along the trajectory in Eq. (4.13). This should be compared to the trajectory of the energy flow towards the horizon in the corresponding trailing–string solution. The latter can be inferred from the results in Refs. [17, 18] : the rate $dE/dt$ for energy flow towards the horizon and the energy density $dE/dr$ per unit length along the dragging string have been there computed as (see[5], e.g., Eqs. (3.19a) and (3.20a) in Ref. [17])

$$\frac{dE}{dt} = \frac{\pi\sqrt{\lambda}\,T^2 v_z^2}{2\sqrt{1-v_z^2}}, \qquad \frac{dE}{dr} = \frac{\sqrt{\lambda}}{2\pi\sqrt{1-v_z^2}R^2}. \tag{5.2}$$

(Recall that $\chi = 2(r_0/r)$ with $r_0 = \pi R^2 T$, and that we consider a situation where $\chi \ll 2$, i.e., $r \gg r_0$.) These expressions involve the 't Hooft coupling $\lambda$, which is inherent in the 'heavy quark' problem (it enters via the string tension, which provides the overall normalization for the Nambu–Goto action, and also for the string energy–momentum tensor) and seems to prevent any comparison to our present results (which correspond to the limit $\lambda \to \infty$). However, the coupling constant disappears in the ratio

$$\frac{dr}{dt} \equiv -\frac{dE/dt}{dE/dr} = -\pi^2 T^2 R^2 v_z^2, \tag{5.3}$$

which determines the trajectory of the energy flow in $AdS_5$, and is the right result to be compared to our respective trajectory in Sect. 4.3. And, indeed, Eq. (5.3), where for the present purposes we can take $v_z \simeq 1$, is identical with our respective expression (4.16), as it can be recognized after a change of variables.

In fact, the identification between our wave solution and the dragging string can be made even more precise: the string world–sheet, as expressed by the function $z(t,r) = v_z t - \zeta(r)$ (the string, which has a shape $z = \zeta(r)$ in the variables $z$ and $r$, moves at constant speed $v_z$, solidary with the heavy quark which is pulled by an external force) is exactly the same as the surface of stationary phase for our Maxwell wave solution $a(t, z, r)$, as computed in Ref. [9]. Specifically,

---

[4]Similarly, for a space–like current, the transition between the moderate–energy and the high–energy regimes, which happens when $\chi_{AB} \sim \chi_{BC}$ (i.e., for $q \sim Q^3/T^2$), is smoothed out by the tunnel effect [9].

[5]The authors of Ref. [17] use the notation $u$ for the radial coordinate in $AdS_5$, which is however not the same as our variable $u$ in Eq. (2.1); rather, their definition for this variable is $u \equiv r/R^2$.

in Ref. [9] we have studied the time–independent version of the above Eq. (4.9), but with a more general form for the potential, valid for all the values of $\chi$ on the right of the 'point of no return', up to $\chi = 2$ (or $r = r_0$). The plane–wave solution has been obtained in the WKB approximation as (see Eq. (D.4) in Appendix D of Ref. [9])

$$a(t,z,r) \approx e^{-i\omega t + iqz} \exp\left\{ i\frac{q}{2\pi T}\left(\frac{1}{2}\ln\frac{r+r_0}{r-r_0} + \arctan\left(\frac{r}{r_0}\right)\right)\right\} . \tag{5.4}$$

(For $r \gg r_0$ and after a change of variables, this expression reduces indeed to the complex exponential part of Eq. (4.11).) The condition of constant phase determines a hypersurface in $AdS_5$ which can be written as $z - (\omega/q)t = \zeta(r) + const.$ where $\omega/q \simeq 1$ is the phase velocity and $\zeta(r)$ is the same function as the shape of the trailing string, cf. Eq. (3.17) of Ref. [17], or Eq. (10) of Ref. [18]. Note the logarithmic singularity in Eq. (5.4) at $r \to r_0$ : this reflects the fact that, as mentioned in Sect. 4.3, the wave–packet can never cross the horizon, but only asymptotically approach to it, according to a law $r - r_0 \propto \exp(-4\pi Tt)$. In the next subsection, we shall propose a physical interpretation for this profile $\zeta(r)$ of the trailing string.

At this point, we should also emphasize an important difference between our present set–up and the 'meson' problem in the previous literature: In the latter, the transverse size $\ell$ of the meson and its longitudinal velocity $v_z$ are independent parameters, so it is in principle possible to choose a velocity $v_z$ arbitrarily close to one (although in practice this meets with the problem of the UV cutoff, as alluded to before [19, 30, 15, 31]). In our approach, the 'meson' is dynamically generated as a fluctuation of the virtual current, which requires a formation time $t \sim t_c$. This introduces an upper limit on the longitudinal momentum $q$ up to which a nearly on–shell 'meson' can form in the plasma: when the 'meson' lifetime $t_f \sim (1/T)\sqrt{q/Q}$ becomes comparable to its formation time $t_c$ — this happens for $q \sim Q^3/T^2$ —, the partonic fluctuation melts in the plasma before having the time to become on–shell. Hence, a 'meson' can form only so far as $q \ll Q^3/T^2$, which in turn introduces an upper limit on the longitudinal velocity $v_z$ of the meson thus generated: $\gamma \ll (Q/T)^2$, or $1 - v_z^2 > (T/Q)^4$. But, of course, there is no corresponding limit on the energy of the current: when $q \gg Q^3/T^2$, the 'point of no return' is reached after the very short time $t_s \sim q/Q_s^2(q) \ll t_c$, and then the current disappears in the plasma before forming a meson. The late–time dynamics which is responsible for this disappearance, as studied in Sect. 4.3, is exactly the same for on–shell or off–shell partonic fluctuations : it is always characterized by the group velocity (4.16) for the falling wave–packet and by the surface of stationary phase surface determined from Eq. (5.4). This points out towards the universality of the dissipation mechanism in a plasma at strong coupling, which is the same for a colorful (heavy or massless) quark as for a (sufficiently energetic) colorless meson or current, although in the AdS/CFT calculation this dynamics may embrace different mathematical descriptions (e.g., a trailing string, or a Maxwell–like wave–packet).

In the next, final, subsection we shall try to elucidate the actual physical mechanism which is responsible for this dissipation in the strongly–coupled gauge theory.

## 5.2 Parton branching at strong coupling

In our physical discussion so far, we have privileged the interpretation in which the time–like current first fluctuates (over a time of the order of the coherence time $t_c \sim q/Q^2$) into a pair

of massless partons which subsequently undergo free motion, along straightline trajectories. In the vacuum, this scenario would hold for ever, and independently of the energy of the current, which only determines the velocities of the particles in the pair. In the plasma, this would hold only for moderately high energies, $q \ll Q^3/T^2$, and for values of $t$ smaller than the time $t_f \sim (1/T)\sqrt{q/Q}$ at which the pair is large enough (in transverse direction) to feel the plasma. But even for larger times $t > t_f$, the partons would still follow classical trajectories, which now describe (in the dual theory) the fall of the Maxwell wave into the black hole. At higher energies, $q \gg Q^3/T^2$, this accelerated fall would show up right away after the early period of diffusion.

Although consistent with our previous calculations and also quite appealing due to its simplicity, this physical picture cannot be fully right, for several reasons: First, at strong coupling, there is no reason why the current should couple to two–parton final states alone, or why these partons should undergo free motion, not even in the vacuum. Rather, the two partons produced in the first, 'electromagnetic', splitting can in turn radiate other partons via strong, 'color', interactions, and also strongly couple to the fluctuations of the vacuum, thus giving rise to a complicated, multi–partonic, final state. Second, the fact that the partons appear to follow classical trajectories in the physical (longitudinal and transverse) space contradicts the quantum nature of the $\mathcal{N} = 4$ SYM theory. Although, in practice, we solve classical equations of motion in the dual gravity theory, the results thus obtained must somehow reflect the quantum nature of the original problem in gauge theory, that should fully reveal itself at strong coupling. This is already manifest in the dynamics at early stages, where our complex exponential in Eqs. (3.12)–(3.13) can be recognized to describe, via the correspondence $\chi \leftrightarrow \pi T L$, *quantum diffusion* (i.e., quantum Brownian motion) in the physical transverse space. There should be a corresponding quantum dynamics hidden in the classical wave solution at later times $t > t_c$, and in what follows we shall try to unveil this dynamics.

This seems *a priori* difficult because of the non–renormalization property of the polarization tensor in the $\mathcal{N} = 4$ SYM theory, as discussed in Sect. 3.1. It is precisely this property which on one hand makes the corresponding result to look so simple at strong coupling (cf. Eq. (3.10)), but on the other hand forbids any direct access to the detailed nature of the final state — and hence to the actual fate of the partons produced by the current. Here, we shall simply try to reconstitute this fate from the dual wave solution via physical considerations, notably, by using the uncertainty principle.

Note first that by using the uncertainty principle alone one can correctly estimate the formation time for the partonic fluctuation, i.e., the coherence time $t_c$ alluded to above. Indeed, in the rest frame of the current, where its 4–momentum reads $q'^\mu = (\omega', 0, 0, 0)$ with $\omega' = Q$, the uncertainty principle requires a fluctuation time $t'_c \gtrsim 1/Q$. This becomes $t_c = \gamma t'_c \sim q/Q^2$ after a Lorentz boost to the frame in which the current is relativistic.

We now turn to later times $t > t_c$ (but lower than $t_f$ in the case of the plasma), where the behavior in Eqs. (3.19)–(3.20) applies, which in turn implies that the partonic system expands in transverse space according to Eq. (3.21). Previously, we have interpreted these results as describing the free motion of two classical particles, but now we shall argue that they are also consistent with *quantum branching at strong coupling*, a dynamics which is much more plausible given the circonstances. In this interpretation, the expansion of the packet in transverse space is the result of the degradation of the partons transverse momentum via successive branching,

in conformity with the uncertainty principle.

Specifically, let us describe the branching process in terms of generations — a kind of mean field picture which should be reasonable at large $N_c$ — and start with a single parton (with longitudinal momentum $q$ and virtuality $Q^2$) at $t_0 = 0$. We shall consider only a $1 \to 2$ splitting vertex, which is representative for the dynamics in a gauge theory. Also, we shall assume that each of the two daughter particles produced in a splitting takes a way, roughly, half of the momentum and virtuality of the parent particle. This assumption is natural at strong coupling, since there there is no need to look for special corners in phase–space, so like collinear or soft emissions, to enhance the probability for splitting. Thus, in the $n$th generation, as obtained after $n \geq 1$ successive branchings, there will be $2^n$ particles, each of them carrying a longitudinal momentum $q_n \simeq q/2^n$ and a virtuality[6] $Q_n \simeq Q/2^n$. Since the virtuality was relatively small to start with ($q \gg Q$), and it further decreases via the splitting, the particles in each generation are nearly on–shell. At strong coupling, a splitting occurs as fast as permitted by the uncertainty principle, so the lifetime of the $(n-1)$-th generation — the time $t_n - t_{n-1}$ necessary to go from the $n-1$ to $n$ branching — can be estimated from the energy imbalance at the splitting vertex. This yields $t_n - t_{n-1} \sim q_n/Q_n^2 \sim 2^n(q/Q^2)$, which rapidly grows with $n$. The time evolution of the virtuality can therefore be estimated as

$$
\frac{Q_n - Q_{n-1}}{t_n - t_{n-1}} \sim -\frac{Q}{q} Q_n^2 \qquad \Longrightarrow \qquad \frac{\mathrm{d}Q(t)}{\mathrm{d}t} \simeq -\frac{Q^2(t)}{\gamma}, \tag{5.5}
$$

where $\gamma = q/Q$ is the Lorentz factor for the original parton. Introducing (by virtue of the uncertainty principle, once again) the transverse size $L_n \sim 1/Q_n$ of the assemble of partons making up the $n$th generation, and similarly $L(t) \sim 1/Q(t)$, we finally obtain

$$
\frac{\mathrm{d}L(t)}{\mathrm{d}t} = \frac{C}{\gamma}, \tag{5.6}
$$

with $C$ a number of order one whose precise value is not under control. This is consistent, as anticipated, with the law (3.21) obtained from the $AdS_5$ calculation via the correspondence $\chi \leftrightarrow \pi T L$. Incidentally, Eq. (5.5) implies $Q(t) \sim \gamma/t$, valid for $t > t_c$.

In the vacuum of the conformal $\mathcal{N} = 4$ SYM theory, this successive branching would hold for ever, down to smaller and smaller values of the longitudinal momentum fraction $z_n = q_n/q_{n-1}$ of the produced partons. If, in order to mimic confinement, the theory is supplemented with an infrared cutoff $\Lambda$ (say, in the form of a cutoff $r_{\min} = \Lambda R^2$ — implying a maximal value $\chi_{\max} \propto 1/\Lambda$ — on the radial distance in the dual string theory), then the splitting will continue until the virtuality of the softest produced partons will become of the order of this cutoff: $Q_N \sim \Lambda$. The total duration of the decay process will then by controlled by the lifetime of the last generation, $t_N - t_{N-1} \sim 2^N(q/Q^2) \sim \gamma/\Lambda$, where we have used $2^N = Q/\Lambda$ and $q/Q = \gamma$. The final partons produced in this process are relatively numerous ($2^N = Q/\Lambda \gg 1$) and have small transverse momenta $q_\perp \sim Q_N \sim \Lambda$, so they will be isotropically distributed in transverse space, within a disk with area $\sim 1/\Lambda^2$ around the longitudinal axis.

But in the case of a plasma, this vacuum–like branching continues only up to a time $t_f \sim \sqrt{\gamma}/T$, when the partonic system has expanded in transverse space up to a size $L_f \sim 1/\sqrt{\gamma}T \ll$

---

[6]As before, the modulus on $Q$ and on $Q_n$ is implicitly understood for time–like partons.

$1/T$. It is easy to understand this 'critical' value in the current scenario: at $t \sim t_f$, the softest partons in the cascade have a typical virtuality $Q_N \sim 1/L_f \sim T\sqrt{\gamma}$ and a longitudinal momentum $q_N = q/2^N \sim \gamma^{3/2}T$. (Here $N$ denotes the number of generations up to a time $t_f$; hence, $2^N \sim QL_f$.) These values satisfy $Q_N^3 \sim q_N T^2$, which is precisely the condition for the partons in this $N$th generation to start interacting with the plasma. In Sect. 4, we have associated this condition with a highly energetic current, which starts to feel the plasma already at early stages during its evolution, before having the time to decay into on–shell partons. Here, we have so far considered a low energy current ($qT^2 \ll Q^3$), which at the beginning decays in the same way as in the vacuum, but whose evolution yields a system of partons for which the condition $Q_N^3 \sim q_N T^2$ is eventually satisfied (since the successive branchings lead to a faster decrease in $Q_n^3$ as compared to $q_n$). The physical meaning of this condition can perhaps be better appreciated by noticing that the rate for the change in virtuality in this $N$th generation (i.e., at time $t \sim t_f$) is of the order

$$\left. \frac{\mathrm{d}Q(t)}{\mathrm{d}t} \right|_{t=t_f} \sim -T^2 \,, \tag{5.7}$$

which looks like a natural order of magnitude for the transverse force exerted by a plasma on colored partons. At a first sight, this might look consistent with a 'quasi–particle' picture for the strongly–coupled plasma, in which the quasi–particles (thermal excitations) have typical momenta $\sim T$ and are randomly distributed in space, with a typical interparticle separation $\sim 1/T$. But then the random scattering between the parton and these quasi–particles would increase the *dispersion* $< p_\perp^2 > - \bar{p}_\perp^2$ in its transverse momentum, rather than uniformly decrease its *average* momentum $\bar{p}_\perp \sim Q$. So, most likely, Eq. (5.7) does not describe thermal scattering, and its precise physical origin remains to be clarified. One should also notice that the partons in this $N$th generation have a relatively long lifetime $\sim \sqrt{\gamma}/T$, so they can lose a significant part of their transverse momentum $|Q_{N+1} - Q_N| \sim T\sqrt{\gamma}$ (before further decaying) even though the respective dissipation rate is rather small, $|\mathrm{d}Q/\mathrm{d}t| \sim T^2$.

For larger times $t > t_f$, the dynamics proceeds in the same way as it would have proceeded at all times $t > 0$ if the current was sufficiently energetic ($q \gtrsim Q^3/T^2$) to start with: namely, the partons keep branching, but this branching is now accelerated by their momentum loss towards the plasma, at an average rate $\sim T^2$. Indeed, as already noticed in relation with Eq. (4.17), the AdS/CFT result (4.16) for the fall of the Maxwell wave into the back hole is tantamount (after the identification $\chi \longleftrightarrow TL \sim T/Q(t)$) to a decelerating transverse force

$$\frac{\mathrm{d}Q(t)}{\mathrm{d}t} \sim -T^2 \,, \tag{5.8}$$

acting on the partons. Because of this force, the partons can now dissociate much faster than in the vacuum : the lifetime $\Delta t_n \sim q_n/Q_n^2$ of a parton from the $n$th generation (with $n > N$) is determined by the condition that, during this time, the parton be able to lose a transverse momentum of order $Q_n$, at a constant rate $\sim T^2$. This condition determines the parton virtuality as $Q_n \sim (q_n T^2)^{1/3}$, which is recognized as the 'saturation momentum' introduced in Sect. 4 — here evaluated for a parton with momentum $q_n \sim q/2^n$. Note that this value for $Q_n$ is considerably larger than $Q/2^n$ (the corresponding value in the vacuum after the same number

of generations), showing that the partons which are involved in this *medium–induced branching* are highly off–shell.

It is also interesting to evaluate the rate $dq/dt$ for longitudinal momentum loss in the plasma, i.e., the longitudinal force acting on the parton. We can write

$$\frac{q_n - q_{n-1}}{t_n - t_{n-1}} \sim -\frac{q_n}{q_n/Q_n^2} \sim -Q_n^2 \qquad \Longrightarrow \qquad \frac{dq(t)}{dt} \simeq -(qT^2)^{2/3}, \qquad (5.9)$$

which is recognized as the 'dynamical' version of the drag force computed in Refs. [17, 18]. Namely, in those papers, one has considered a heavy quark moving through the plasma at a constant speed $v_z$ and found that, in order to compensate for its energy loss, one needs to drag this quark with a constant force $dp/dt = (1/v_z)(dE/dt)$ that can be read off the first equation (5.2). Therefore[7] $dp/dt \propto \gamma T^2$, where $\gamma = 1/\sqrt{1 - v_z^2}$ is time–independent in the context of Refs. [17, 18]. Our force (5.9) can be rewritten in a formally similar way by introducing the Lorentz factor for the (virtual) parton as $\gamma(t) = q(t)/Q(t)$ — which however is now time–dependent, because of the uncompensated energy loss — and recalling that, for this parton, $Q(t) = Q_s(q(t)) \sim (qT^2)^{1/3}$, so that we indeed have $(qT^2)^{2/3} \sim \gamma(t)T^2$.

Eq. (5.9) tells us that a parton (or current) will totally lose its energy over a time interval $t_{\rm loss} \sim (1/T)(q_N/T)^{1/3}$, with $q_N$ the value of its longitudinal momentum at the time where that parton (or current) has started to feel the plasma. For an $\mathcal{R}$–current with moderately high energy ($qT^2 \ll Q^3$), we have seen that $q_N \sim \gamma^{3/2}T$, which in turn implies $t_{\rm loss} \sim \sqrt{\gamma}/T$, in agreement with the respective AdS/CFT result in Eq. (4.5). But for a very energetic current ($qT^2 \gg Q^3$), and also for a colored parton with any energy, $q_N$ is the same as its original momentum at $t = 0$, and then we find $t_{\rm loss} \sim (1/T)(q/T)^{1/3}$, in agreement with the corresponding result in Eq. (4.7) and also with a very recent result in Ref. [16].

We shall conclude this discussion with a physical interpretation for the trailing string solution originally obtained in Refs. [17, 18] (and which, we recall, also emerges from our Maxwell wave solution, cf. Eq. (5.4)). Namely, we shall argue that the function $\zeta(r)$ which defines the shape of the string is 'dual', via the identification $r/R^2 \leftrightarrow 1/L$, to the enveloping curve of the parton distribution created via branching in the medium. This curve can be best visualized if one considers a stationary situation similar to that in Refs. [17, 18], namely the situation in which some external force is continuously giving energy to the system, in such a way that the leading particle propagates at constant speed $v_z \lesssim 1$. The 'leading particle' is either our $\mathcal{R}$–current in the high–energy regime at $qT^2 \gg Q^3$, or some colored parton like the heavy quark considered in [17, 18]. This particle creates a parton cascade via successive branchings and the average (gross) properties of this cascade are independent of time. The parton distribution being roughly isotropic in transverse space, as argued before, we can focus on a particular plane, say, $(x, z)$ (see Fig. 4). The enveloping curve of the distribution is then the function $\Delta z(L)$ which relates the longitudinal separation $\Delta z$ between a parton in this plane and the leading particle to the transverse width $L$ of the cascade at the position of that parton. To construct this function, it is convenient to return to the description of the parton cascade in terms of generations; this

---

[7]We take $v_z \simeq 1$, as appropriate for comparing to our present calculations.
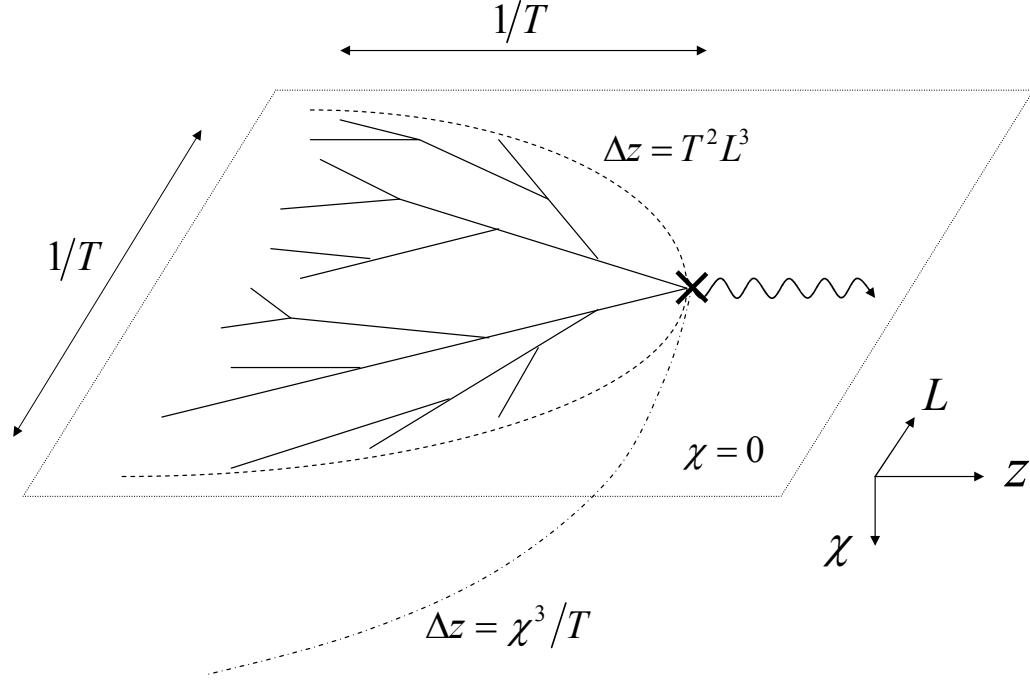
**Figure 4:** *The parton cascade generated by the current via medium–induced branching in the physical Minkowski space (represented here as the boundary of $AdS_5$ at $\chi = 0$) and the trailing string attached to the leading particle (represented for $\chi \ll 1$). The latter is 'dual' to the enveloping curve of the former.*

implies

$$\Delta z(L_n) \simeq \sum_{j=1}^{n} (1 - v_j)\Delta t_j \,, \tag{5.10}$$

where $L_n \simeq 1/Q_n$ and where $Q_j$, $\Delta t_j$, and $v_j$ denote, respectively, the typical virtuality, lifetime, and velocity of a parton from the $j$th generation, with $j \leq n$. According to the previous discussion, we have $Q_j \sim (q_j T^2)^{1/3}$, $\Delta t_j \sim q_j/Q_j^2$, and

$$v_j \simeq \frac{q_j}{\omega_j} = \frac{q_j}{\sqrt{Q_j^2 + q_j^2}} \simeq 1 - \frac{Q_j^2}{2q_j^2} \,. \tag{5.11}$$

Therefore,

$$\Delta z(L_n) \sim \sum_{j=1}^{n} \frac{1}{q_j} \simeq \int_0^n \mathrm{d}j \, \frac{1}{q(j)} \simeq \int_0^{L_n} \frac{\mathrm{d}L}{L} T^2 L^3 \sim T^2 L_n^3 \,, \tag{5.12}$$

where we have used $\mathrm{d}j \simeq \mathrm{d}L_j/L_j$ (since $\mathrm{d}(\ln L_j) \simeq -(1/3)\mathrm{d}(\ln q_j) \sim \mathrm{d}j$; we recall that $q^j = q/2^j$). We thus have found that $\Delta z(L) \sim T^2 L^3$. After replacing $L \to R^2/r$ within this result (in order to compare with the shape $\zeta(r)$ of the trailing string), we finally deduce $\Delta z(r) \sim T^2(R^6/r^3)$. As anticipated, this is parametrically the same as the expansion of the function $\zeta(r)$ for $r \gg r_0$ (where our present calculation is supposed to apply).

By inverting the function above, we find that $L$ grows with $\Delta z$ as $L \sim (\Delta z/T^2)^{1/3}$. This is correct so long as $L$ remains smaller than $1/T$, and hence for values of $\Delta z$ which are themselves smaller than $1/T$. But the transverse width of the partonic distribution is roughly limited[8] to $L \lesssim 1/T$, since partons with momenta $Q \lesssim T$ disappear in the thermal bath. This argument suggests that at larger distances $\Delta z \gtrsim 1/T$ the parton distribution should approach a cylinder with diameter $L \sim 1/T$ (see Fig. 4). This is again similar to the corresponding behavior of the trailing string, which for $\zeta \gtrsim 1/T$ approaches asymptotically the horizon at $r = r_0$ [17, 18].

This 'duality' between the shape of the trailing string and the enveloping curve of the parton distribution implies a similar duality between our Maxwell wave in $AdS_5$ and the wave which would describe the physical parton distribution in Minkowski space. Namely, the latter can be obtained by replacing $r \to 2R^2/L$ in Eq. (5.4), thus yielding

$$a(t, z, L) \approx e^{-i\omega t + iqz + iq\Delta z(L)},$$

$$\Delta z(L) \equiv \frac{L_0}{4}\left[\frac{1}{2}\ln\frac{L_0 + L}{L_0 - L} + \arctan\left(\frac{L_0}{L}\right)\right], \qquad L_0 \equiv \frac{2}{\pi T}. \qquad (5.13)$$

The phase of this wave is stationary along a paraboloid in Minkowski space which represents the enveloping surface of the parton distribution. The fact that this distribution can be characterized by its enveloping curve alone (i.e., that is does not depend separately upon the transverse coordinates $x$ and $y$, with $x, y \leq L$, but only upon the points on a circle with radius $L$) can be simply understood in physical terms: all the points in a transverse cross–section of this paraboloid at a fixed value $\Delta z \equiv z - (\omega/q)t$ correspond to partons which belong to a same generation. Such partons move in phase with each other, as they have the same velocity. Accordingly, the phase of the wave must be the same for all such points, as indeed happens for the wave in Eq. (5.13).

## Acknowledgments

## A. Wave–packet evolution in the vacuum

In this Appendix we shall consider the initial value problem for the Schrödinger–like equation (3.11) in a slightly more systematic way, by using the *Ansatz* (2.12) in order to search for

---

[8]Actually, as pointed out in Refs. [32, 33, 34], the energy and momentum transfer from the leading particle can also induce longer range ($L \gg 1/T$) perturbations into the plasma, so like sound waves or Mach cones. But in order to see such perturbations, one has to take into account the feedback of the trailing string, or of the Maxwell wave, on the $AdS_5$–Schwarzschild geometry, something that goes beyond the purpose of this work.

appropriate solutions. We recall that we are interested in solutions $\psi(\tilde{t}, \chi)$ which for $\tilde{t}$ are localized near $\chi = 0$. The precise form of the initial condition is however irrelevant, and in what follows it will be more convenient (since mathematically simpler) not to stick to a particular initial condition, but rather identify a particular solution and then verify that this solution satisfies indeed the condition of localization at early times ($\tilde{t} \to 0$).

We consider the time–like case, i.e., we take the minus sign in front of $K^2$ in Eq. (3.11), since this is the most interesting case. After inserting the *Ansatz* (2.12) into Eq. (3.11), one can recognize the Bessel equation for $\Psi(\varepsilon, \chi)$, up to some trivial changes of function and variable. An interesting particular solution is

$$\psi(\tilde{t}, \chi) = \int d\varepsilon \, e^{-i\varepsilon\tilde{t} - \frac{\varepsilon^2}{2\sigma^2}} \sqrt{\chi} \, J_0(\chi\sqrt{K^2 + 2k\varepsilon}) \,, \tag{A.1}$$

where the reason for choosing the particular Bessel function $J_0$ (rather than the most general combination $c_1 J_0 + c_2 N_0$) should become clear in a moment. We shall estimate the above integral separately for small and, respectively, large values for the external coordinates $\tilde{t}$ and $\chi$ — the change in behavior occurring at $\tilde{t} \sim \tilde{t}_c \simeq 2k/K^2$ (the coherence time) and for $\chi \sim \chi_c \simeq 1/2K$ (the position of the wave–packet at $\tilde{t} = \tilde{t}_c$). In this analysis, one should keep in mind that the width $\sigma$ of the packet obeys to Eq. (2.13).

Specifically, for small times $\tilde{t} \ll \tilde{t}_c$ (with $\tilde{t} \gtrsim 1/\sigma$ though) and for $\chi \ll \chi_c$, the integral is dominated by energies $\varepsilon$ such that $K^2/2k \ll \varepsilon \ll \sigma$, as we shall shortly check. Then one can neglect the Gaussian factor inside the integrand and also the $K^2$ term inside the argument of the Bessel function. The resulting integral can be performed exactly (see formula 6.631-6 in Ref. [35]), and reproduces the corresponding solution found in Sect. 3.2 (cf. Eq. (3.12)) :

$$\psi \simeq \int_0^\infty d\varepsilon \, e^{-i\varepsilon\tilde{t}} \sqrt{\chi} \, J_0(\chi\sqrt{2k\varepsilon}) = \frac{-i\sqrt{\chi}}{\tilde{t}} e^{i\frac{k\chi^2}{2\tilde{t}}} \,. \tag{A.2}$$

In fact, it was precisely this possibility, to exactly perform the above integration, which motivated our choice for the Bessel function $J_0$ in Eq. (A.1).

As discussed in Sect. 3.2, this solution implies that the energy diffuses along a trajectory $\chi \sim \sqrt{\tilde{t}/k}$. For values of $\chi$ along, or near, this trajectory, we have $\chi\sqrt{2k\varepsilon} \sim \sqrt{\tilde{t}\varepsilon}$, and then the integral in Eq. (A.2) is controlled by $\varepsilon \sim 1/\tilde{t}$ (since this is the only scale inside the integrand). Hence, for $\tilde{t} \ll \tilde{t}_c$, we have $\varepsilon \gg K^2/2k$, as anticipated. Since, moreover, the time variable is restricted to $\tilde{t} \gtrsim 1/\sigma$, the condition that $\varepsilon \ll \sigma$ is satisfied as well.

In the other interesting case, namely for relatively large times and radial coordinates, $\tilde{t} \gg \tilde{t}_c$ and $\chi \gg \chi_c$, the integral in Eq. (A.1) is dominated by relatively small values of $\varepsilon$, such that $2k\varepsilon \ll K^2$. Moreover, in this regime we have $K\chi \gg 1$, so one can use the asymptotic expression for the Bessel function, to obtain

$$\psi \sim \int d\varepsilon \, e^{-i\varepsilon\tilde{t} - \frac{\varepsilon^2}{2\sigma^2} + i\chi\sqrt{K^2 + 2k\varepsilon}} \,, \tag{A.3}$$

where we have kept only the outgoing–wave component of the solution. (The other component would yield a solution propagating from the bulk towards the boundary.) The dominant contribution can now be obtained by expanding the square root in the exponent to linear order in $\varepsilon$

and then performing a Gaussian integral :

$$\int \mathrm{d}\varepsilon \, \mathrm{e}^{-i\varepsilon\tilde{t}-\frac{\varepsilon^2}{2\sigma^2}+iK\chi+i\frac{k\chi}{K}\varepsilon} \sim \mathrm{e}^{iK\chi-\frac{\sigma^2}{2}\left(\tilde{t}-\frac{k}{K}\chi\right)^2} . \tag{A.4}$$

The strength $|\psi|$ of the wave, which shows where the energy is located, has a peak at $\tilde{t} = (k/K)\chi$. Hence, this solution represents a wave–packet with propagates in $AdS_5$ with constant group velocity :

$$\chi = v_g\tilde{t}, \qquad v_g = \frac{K}{k} = \frac{1}{\gamma} = \sqrt{1 - v_z^2} , \tag{A.5}$$

in agreement with the simpler analysis in Sect. 3.2.

## B. Classical particle falling in AdS

In this appendix we consider the motion of a classical pointlike particle falling down into the $AdS_5$ black hole and compare its motion to the propagation of a time–like current, as previously studied in Sect. 4. (See Ref. [36] for a similar study.)

A massless particle propagates along a null geodesics

$$0 = \mathrm{d}s^2 \propto -\left(1 - \frac{\chi^4}{\chi_H^4}\right)\mathrm{d}t^2 + \mathrm{d}x^2 + \mathrm{d}y^2 + \mathrm{d}z^2 + \frac{\mathrm{d}\chi^2}{(2\pi T)^2\left(1 - \frac{\chi^4}{\chi_H^4}\right)} , \tag{B.1}$$

where $\chi_H = 2$. For a particle with velocity (the variables $q$ and $\omega$ are introduced below to facilitate the comparison with the discussion in Sect. 4)

$$v = \frac{\mathrm{d}z}{\mathrm{d}t} \equiv \frac{q}{\omega} , \tag{B.2}$$

in the $z$–direction, (B.1) reads

$$\left(\frac{\mathrm{d}\chi}{\mathrm{d}\tilde{t}}\right)^2 = \left(1 - \frac{\chi^4}{\chi_H^4}\right)\left(1 - \frac{\chi^4}{\chi_H^4} - v^2\right) . \tag{B.3}$$

In the static case, $v = 0$, one can integrate explicitly

$$\tilde{t} = \tanh^{-1}\frac{\chi}{\chi_H} + \tan^{-1}\frac{\chi}{\chi_H} . \tag{B.4}$$

The particle reaches near the horizon $\chi \sim \chi_H$ in time $t \sim 1/T$. This is indeed similar to the evolution of a time–like current with $q = 0$.

When $q \neq 0$, (B.3) can be rewritten as

$$\left(\frac{\mathrm{d}\chi}{\mathrm{d}\tilde{t}}\right)^2 = \left(1 - \frac{\chi^4}{\chi_H^4}\right)\left(\frac{|Q^2|}{\omega^2} - \frac{\chi^4}{\chi_H^4}\right) . \tag{B.5}$$

When $1 \gg Q/\omega \gg \chi^2/\chi_H^2$, or

$$\chi \ll 2\sqrt{\frac{Q}{q}} \sim \chi_v \tag{B.6}$$

one easily finds

$$\frac{\mathrm{d}\chi}{\mathrm{d}\tilde{t}} \simeq \frac{Q}{\omega}\,, \tag{B.7}$$

which is equivalent to Eq. (3.20). This is valid until a time

$$t \lesssim \frac{1}{T}\sqrt{\frac{\omega}{Q}} \sim t_f\,, \tag{B.8}$$

when the 'point of no return' $\chi \sim \chi_v$ is reached. The above estimates for $t_f$ and $\chi_v$ are indeed consistent with the corresponding ones derived from the current dynamics in Sect. 4 (where $\chi_v$ was rather denoted as $\chi_{BC}$). Therefore, the intermediate stage of the evolution of a time–like, moderate energy ($q \ll Q^3/T^2$), 'photon' looks indeed like a massless pointlike particle falling into the bulk. On the other hand, the initial, diffusive regime of the photon evolution has no classical analog. Moreover, a pointlike particle stalls in the $\chi$ direction at $\chi \sim \chi_f$, as clear by inspection of Eq. (B.5), whereas a photon (string) keeps on falling further into the bulk as discussed in the main text.

## References

[1] M. Gyulassy and L. McLerran, "New forms of QCD matter discovered at RHIC," *Nucl. Phys.* **A750** (2005) 30–63, `nucl-th/0405013`.

[2] B. Muller, "From Quark-Gluon Plasma to the Perfect Liquid," *Acta Phys. Polon.* **B38** (2007) 3705–3730, `arXiv:0710.3366 [nucl-th]`.

[3] D. T. Son and A. O. Starinets, "Viscosity, Black Holes, and Quantum Field Theory," *Ann. Rev. Nucl. Part. Sci.* **57** (2007) 95–118, `arXiv:0704.0240 [hep-th]`.

[4] J. M. Maldacena, "The large N limit of superconformal field theories and supergravity," *Adv. Theor. Math. Phys.* **2** (1998) 231–252, `hep-th/9711200`.

[5] S. S. Gubser, I. R. Klebanov, and A. M. Polyakov, "Gauge theory correlators from non-critical string theory," *Phys. Lett.* **B428** (1998) 105–114, `hep-th/9802109`.

[6] E. Witten, "Anti-de Sitter space, thermal phase transition, and confinement in gauge theories," *Adv. Theor. Math. Phys.* **2** (1998) 505–532, `hep-th/9803131`.

[7] D. Anselmi, D. Z. Freedman, M. T. Grisaru, and A. A. Johansen, "Nonperturbative formulas for central functions of supersymmetric gauge theories," *Nucl. Phys.* **B526** (1998) 543–571, `hep-th/9708042`.

[8] S. Caron-Huot, P. Kovtun, G. D. Moore, A. Starinets, and L. G. Yaffe, "Photon and dilepton production in supersymmetric Yang- Mills plasma," *JHEP* **12** (2006) 015, `hep-th/0607237`.

[9] Y. Hatta, E. Iancu, and A. H. Mueller, "Deep inelastic scattering off a N=4 SYM plasma at strong coupling," *JHEP* **01** (2008) 063, `arXiv:0710.5297 [hep-th]`.

[10] K. Peeters, J. Sonnenschein, and M. Zamaklar, "Holographic melting and related properties of mesons in a quark gluon plasma," *Phys. Rev.* **D74** (2006) 106008, `hep-th/0606195`.

[11] H. Liu, K. Rajagopal, and U. A. Wiedemann, "An AdS/CFT calculation of screening in a hot wind," *Phys. Rev. Lett.* **98** (2007) 182301, `hep-ph/0607062`.

[12] M. Chernicoff, J. A. Garcia, and A. Guijosa, "The energy of a moving quark-antiquark pair in an N = 4 SYM plasma," *JHEP* **09** (2006) 068, `hep-th/0607089`.

[13] E. Caceres, M. Natsuume, and T. Okamura, "Screening length in plasma winds," *JHEP* **10** (2006) 011, `hep-th/0607233`.

[14] S. D. Avramis, K. Sfetsos, and D. Zoakos, "On the velocity and chemical-potential dependence of the heavy-quark interaction in N = 4 SYM plasmas," *Phys. Rev.* **D75** (2007) 025009, `hep-th/0609079`.

[15] H. Liu, K. Rajagopal, and U. A. Wiedemann, "Wilson loops in heavy ion collisions and their calculation in AdS/CFT," *JHEP* **03** (2007) 066, `hep-ph/0612168`.

[16] S. S. Gubser, D. R. Gulotta, S. S. Pufu, and F. D. Rocha, "Gluon energy loss in the gauge-string duality," `arXiv:0803.1470 [hep-th]`.

[17] C. P. Herzog, A. Karch, P. Kovtun, C. Kozcaz, and L. G. Yaffe, "Energy loss of a heavy quark moving through N = 4 supersymmetric Yang-Mills plasma," *JHEP* **07** (2006) 013, `hep-th/0605158`.

[18] S. S. Gubser, "Drag force in AdS/CFT," *Phys. Rev.* **D74** (2006) 126005, `hep-th/0605182`.

[19] H. Liu, K. Rajagopal, and U. A. Wiedemann, "Calculating the jet quenching parameter from AdS/CFT," *Phys. Rev. Lett.* **97** (2006) 182301, `hep-ph/0605178`.

[20] J. Casalderrey-Solana and D. Teaney, "Transverse momentum broadening of a fast quark in a N = 4 Yang Mills plasma," *JHEP* **04** (2007) 039, `hep-th/0701123`.

[21] J. Casalderrey-Solana and D. Teaney, "Heavy quark diffusion in strongly coupled N = 4 Yang Mills," *Phys. Rev.* **D74** (2006) 085012, `hep-ph/0605199`.

[22] J. Polchinski and M. J. Strassler, "Deep inelastic scattering and gauge/string duality," *JHEP* **05** (2003) 012, `hep-th/0209211`.

[23] Y. Hatta, E. Iancu, and A. H. Mueller, "Deep inelastic scattering at strong coupling from gauge/string duality : the saturation line," *JHEP* **01** (2008) 026, `arXiv:0710.2148 [hep-th]`.

[24] D. M. Hofman and J. Maldacena, "Conformal collider physics: Energy and charge correlations," `arXiv:0803.1467 [hep-th]`.

[25] D. T. Son and A. O. Starinets, "Minkowski-space correlators in AdS/CFT correspondence: Recipe and applications," *JHEP* **09** (2002) 042, `hep-th/0205051`.

[26] G. R. Farrar, H. Liu, L. L. Frankfurt, and M. I. Strikman, "Transparency in Nuclear Quasiexclusive Processes with Large Momentum Transfer," *Phys. Rev. Lett.* **61** (1988) 686–689.

[27] Y. L. Dokshitzer, V. A. Khoze, A. H. Mueller, and S. I. Troian, "Basics of perturbative QCD,". Gif-sur-Yvette, France: Ed. Frontieres (1991) 274 p. (Basics of).

[28] C. P. Herzog, "Energy loss of heavy quarks from asymptotically AdS geometries," *JHEP* **09** (2006) 032, `hep-th/0605191`.

[29] E. Caceres and A. Guijosa, "Drag force in charged N = 4 SYM plasma," *JHEP* **11** (2006) 077, `hep-th/0605235`.

[30] P. C. Argyres, M. Edalati, and J. F. Vazquez-Poritz, "No-drag string configurations for steadily moving quark- antiquark pairs in a thermal bath," *JHEP* **01** (2007) 105, `hep-th/0608118`.

[31] P. C. Argyres, M. Edalati, and J. F. Vazquez-Poritz, "Lightlike Wilson loops from AdS/CFT," `arXiv:0801.4594 [hep-th]`.

[32] S. S. Gubser, S. S. Pufu, and A. Yarom, "Energy disturbances due to a moving quark from gauge-string duality," *JHEP* **09** (2007) 108, `arXiv:0706.0213 [hep-th]`.

[33] P. M. Chesler and L. G. Yaffe, "The wake of a quark moving through a strongly-coupled $\mathcal{N} = 4$ supersymmetric Yang-Mills plasma," *Phys. Rev. Lett.* **99** (2007) 152001, `arXiv:0706.0368 [hep-th]`.

[34] P. M. Chesler and L. G. Yaffe, "The stress-energy tensor of a quark moving through a strongly-coupled N=4 supersymmetric Yang-Mills plasma: comparing hydrodynamics and AdS/CFT," `arXiv:0712.0050 [hep-th]`.

[35] I. Gradshteyn and I. Ryzhik, "Table of Integrals, Series, and Products,". 4th Edition, Academic Press, Boston, USA (1994).

[36] S.-J. Sin and I. Zahed, "Holography of radiation and jet quenching," *Phys. Lett.* **B608** (2005) 265–273, `hep-th/0407215`.